Westinghouse ENGINEER

July 1969

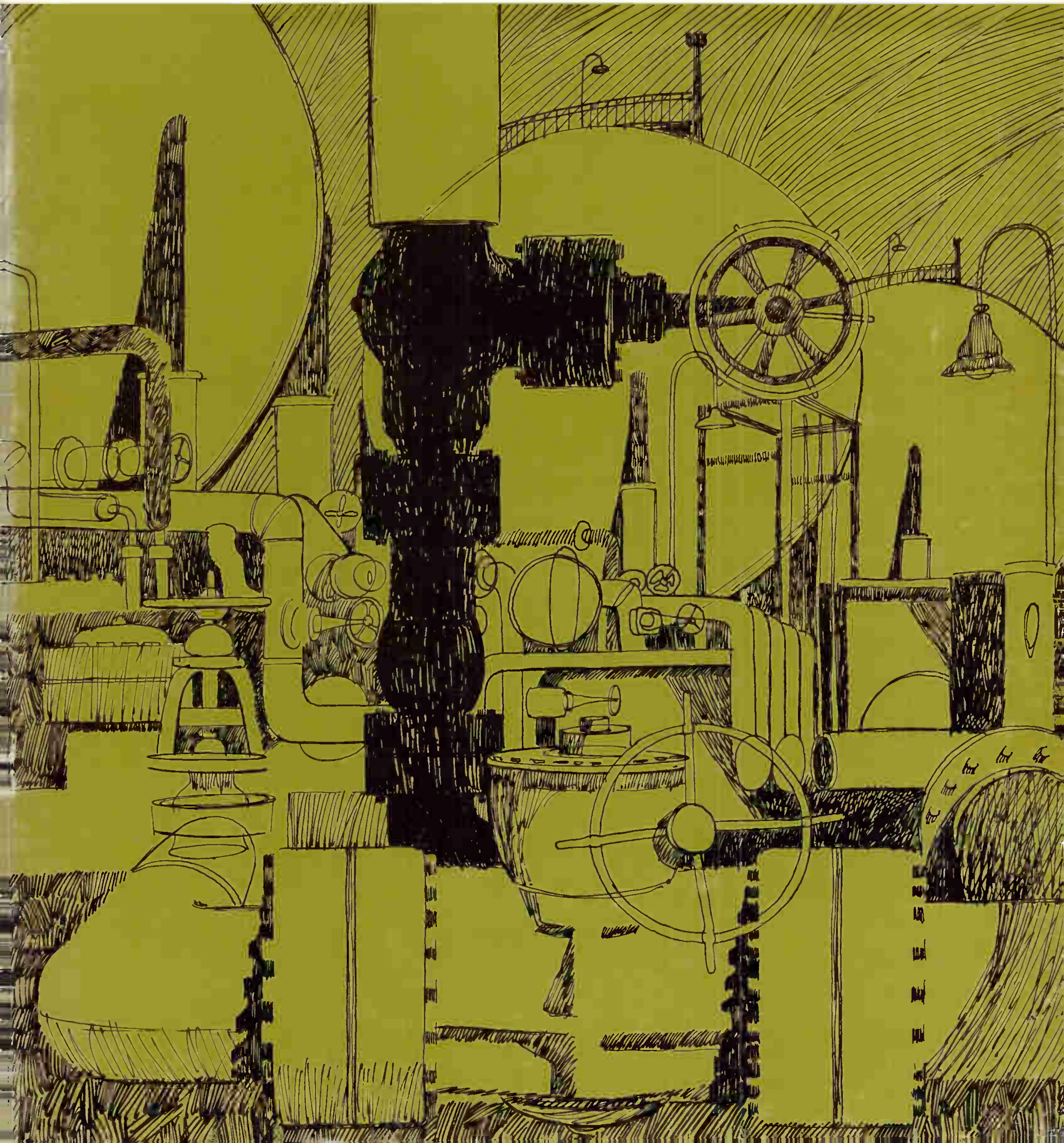

Large Generator Rotors Tested

The large turbine-generator rotor at right is being lowered into a test facility that tests and balances rotors at speeds above the normal values of 1800 and 3600 r/min, respectively, for four-pole and two-pole rotors. Four-pole rotors weigh up to 250 tons and are about six feet in diameter, while the two-pole rotors weigh up to 100 tons with diameters of about four feet.

Walls and cover plates of the facility are made of thick reinforced concrete to contain the pieces if a rotor breaks due to the high rotational stresses at overspeed. Cover plates weigh 50 tons each and are seven feet thick.

The test facility has two drive motors, one 5000-hp ac and the other 2000-hp dc. It is located at the Westinghouse Large Rotating Apparatus Division, East Pittsburgh, Pennsylvania.

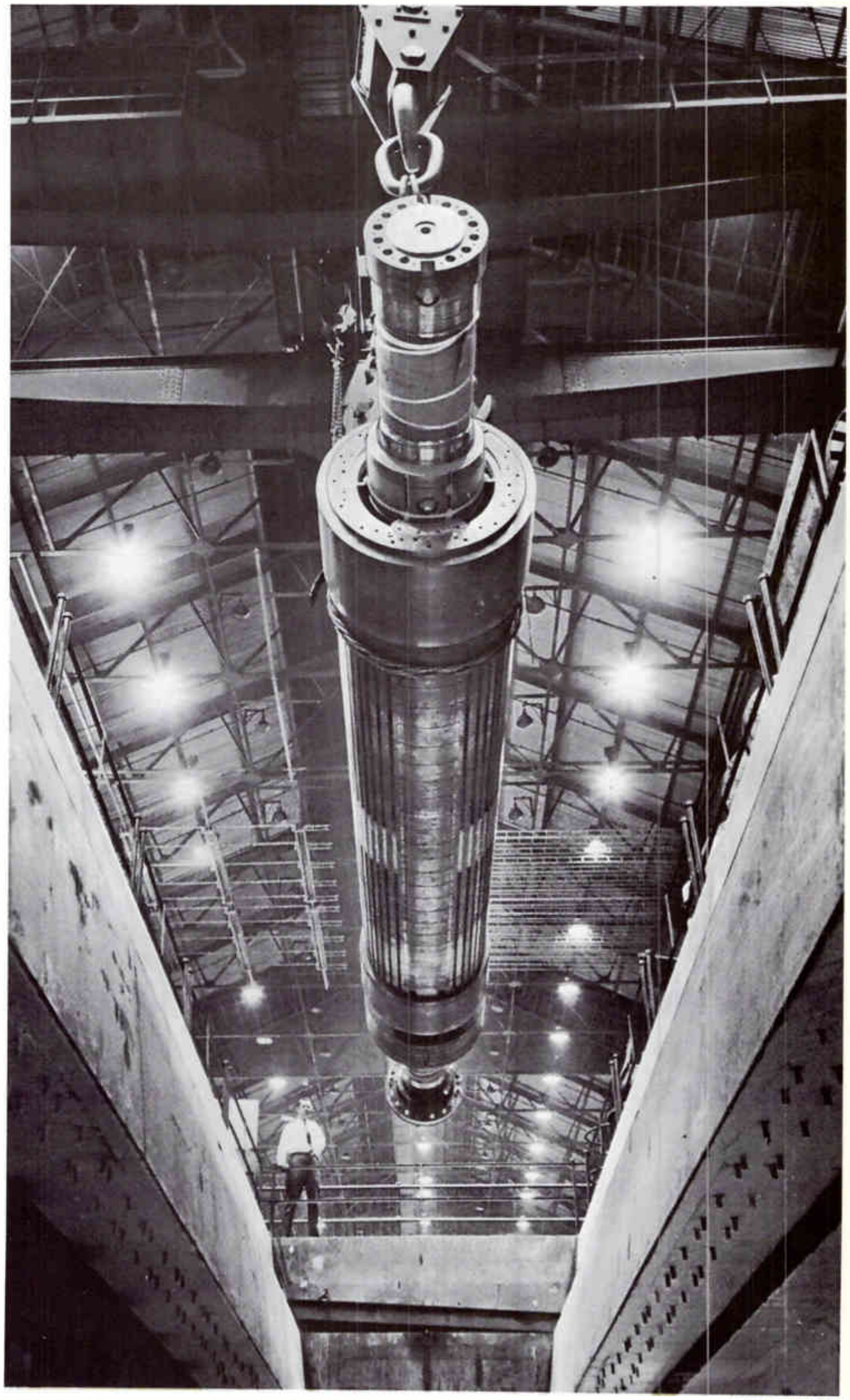

Westinghouse ENGINEER
July 1969, Volume 29, Number 4

5.00
Engineering
36819

Subscriptions: United States and possessions, $2.50 per year; all other countries, $3.00 per year. Single copies, 50¢ each.

Mailing address: Westinghouse ENGINEER, P. O. Box 2278, 3 Gateway Center, Pittsburgh, Pennsylvania 15230.

Published bimonthly by the Westinghouse Electric Corporation, Pittsburgh, Pennsylvania. Printed in the United States by The Lakeside Press, Lancaster, Pennsylvania. Reproductions of the magazine by years are available on positive microfilm from University Microfilms, Inc., 300 North Zeeb Road, Ann Arbor, Michigan 48106.

Cover design: Process industries are suggested in the cover design by Tom Ruddy. The article beginning on the following page describes direct digital control, which is applicable to the process industries and also to various utility control problems.

Direct Digital Control Comes of Age

Calvin W. Eggers

Properly applied, direct digital control can provide otherwise unattainable (or uneconomic) control flexibility and performance.

Dynamic control of processes was long the province of analog control loops, and when digital control computers were first applied for process optimizing they were arranged to output set points to conventional analog controllers. While such set-point (or supervisory) control is still an important part of the control spectrum, it has now been supplemented by direct digital control (DDC).

In DDC, the digital computer sends control signals directly to the process actuators instead of to an intermediate controller. The obvious benefit is elimination of some conventional control equipment, but often of more value is the greater design flexibility and improved control.

The DDC computer is able to do the job of an analog controller by use of a mathematical representation of the control equations. For example, to achieve proportional plus integral control, the computer calculates the error and the integral of the error on the basis of periodic samples of the variable being controlled. The combination of the two terms with their gain settings is the output to the actuator. (See *DDC Fundamentals*, page 102.) The computer calculations that effect direct digital control are referred to as algorithms.

The foregoing simple example, of course, only shows how to do an average job of control with a relatively expensive computer—a job that could be done just as well with an inexpensive controller. The justification for DDC is that, in a real application, *one computer does the job of many controllers* by multiplexing (Fig. 1). Inputs are read one at a time, calculations are made one at a time, and outputs are set one at a time.

Multiplexing is possible because control calculations for a single loop take only a small percentage of the computer's time. The algorithm for each control loop is repeated at intervals (the sampling rate) that depend on the type of loop. (Examples are: flow, 1 second; pressure or level, 5 seconds; temperature, 20 seconds.) The Prodac 50 computer system can do the calculations for as many as 80 typical loops every second; the Prodac 2000 and Prodac 250 are even faster, calculating for several hundred loops every second.

Calvin W. Eggers is Manager, General System Engineering, Hagan/Computer Systems Division, Westinghouse Electric Corporation, Pittsburgh, Pennsylvania.

Why DDC

DDC should be considered when a computer is already planned for some other function, when there are many control loops, or when special and complex equipment would be required to implement the control without a computer. Of the many reasons for considering DDC, none provides a clear-cut decision in every situation. Rather, they are things to consider in evaluating what combination of digital and analog control should be used.

Technical Reasons—Design flexibility is greater, so it is often possible to experiment with the system. For example, the user can try a loop with and without feedforward control for some other variable or with and without derivative control—all without moving a wire or pipe or adding a piece of equipment.

Control performance can be better, since DDC can do things that are impossible or require additional equipment in analog systems. Examples of nonlinear operations that are possible include multiplication or division of two variables, selection of the highest or lowest of two or more variables, and generating arbitrary nonlinear functions of a given variable. Another useful tool is automatic selection of the best control setting, depending on operating level.

Operation is safe and consistent. The DDC computer includes programs to check variables against high and low limits, so, if a sensor fails, the operator is alerted and the bad value is not stored as the basis for control. Also, computers seldom develop erratic failures that degrade control performance; once debugged, the calculations for each loop stay consistent.

Economic Reasons—Less capital equipment is required, because one computer replaces many analog controllers and associated equipment. Although a break-even point is hard to identify, obviously replacement of analog equipment can pay for part of a computer. The tradeoff depends very much on the complexity of control and the associated analog equipment costs. Other economic and technical reasons must be considered for the rest of the justification. Some of the economic reasons are:

1) Reduced staffing. The centralized DDC system may reduce operator requirements from what is needed with many scattered control stations.

2) Reduced maintenance. Although different talent is required to maintain a computer, it is just one piece of equipment instead of many analog controllers each requiring individual attention.

3) Improved operation. DDC can improve quality, reduce raw material, or increase production in some processes. The improvements might be from faster setup, closer regulation, or making indirect measurements not possible with analog control.

Reliability Considerations—A common objection to DDC is, "If an analog controller fails, we lose one loop; if the computer fails, we lose all the control." The objection is valid, although the reliability of computers is good and constantly improving. Possible compromises (all of which hurt the economic advantage) are provision of simple analog loops as backup for complex digital loops; manual controls for periods of computer outage, with selected analog backup loops; and two computers, one backing up the other. The current tendency is toward the second alternative.

DDC Hardware

The hardware required to close a DDC loop consists of a transducer, computer input, computer central processor unit (CPU), computer output, actuator, and operator communication device (Fig. 1). The transducer, or sensor, is no different from that in conventional control; it usually produces an analog millivolt or milliampere signal. The computer input subsystem, which converts the measured signal into a form usable by the central processor, is usually a multiplexer and an analog-to-digital convertor designed to read all inputs of the system in sequence.

Selection of the computer central processor is based on two criteria—memory size and speed. The memory size required is determined by such factors as whether the computer is dedicated to DDC or includes other programs, how many DDC loops there are, how many parameters per loop, how many different types of controllers, and whether the programs allow modification of control loops and other flexibility. Westinghouse DDC applications vary in size from a Prodac 50 with 8192 words of core memory to a Prodac 250 with 24,576 words of core memory and 375,000 words of mass memory. The speed required is determined by whether the computer is dedicated to DDC or is executing other programs as well; if the latter, what percentage of time is allocated to DDC; and how many loops must be serviced per second.

The computer output and the actuator must be considered together. One simple arrangement is for the computer to provide raise-lower or open-close contacts to a process device, say a motor-operated valve; another is to make the output a resistive ladder driving a current-to-pressure convertor, the actuator, and finally the valve. If back-up or manual intervention is required, a typical system has a manual station for each loop, driven by the computer and in turn driving the actuator. Multiplexing is used to share one analog output for several stations, and the stations have track-hold circuits that keep the actuator and valve at the last position in the event of a computer outage.

Functional Specification—In developing each application, the many hardware variables and design decisions that are possible must be considered along with the software (programs) to be used, because both hardware and software enter into functional tradeoffs. Basic questions have to be answered in these areas:

1) Loop timing. What is the fastest loop sampling rate required? Are all loops sampled at the same rate? Do the sampling rates have to be changed on line?

2) Loop speed. How many loops must be serviced per second? Is this compatible with planned CPU speed?

3) Loop construction. Is the ability to hook up routine loops with standard controllers desired?

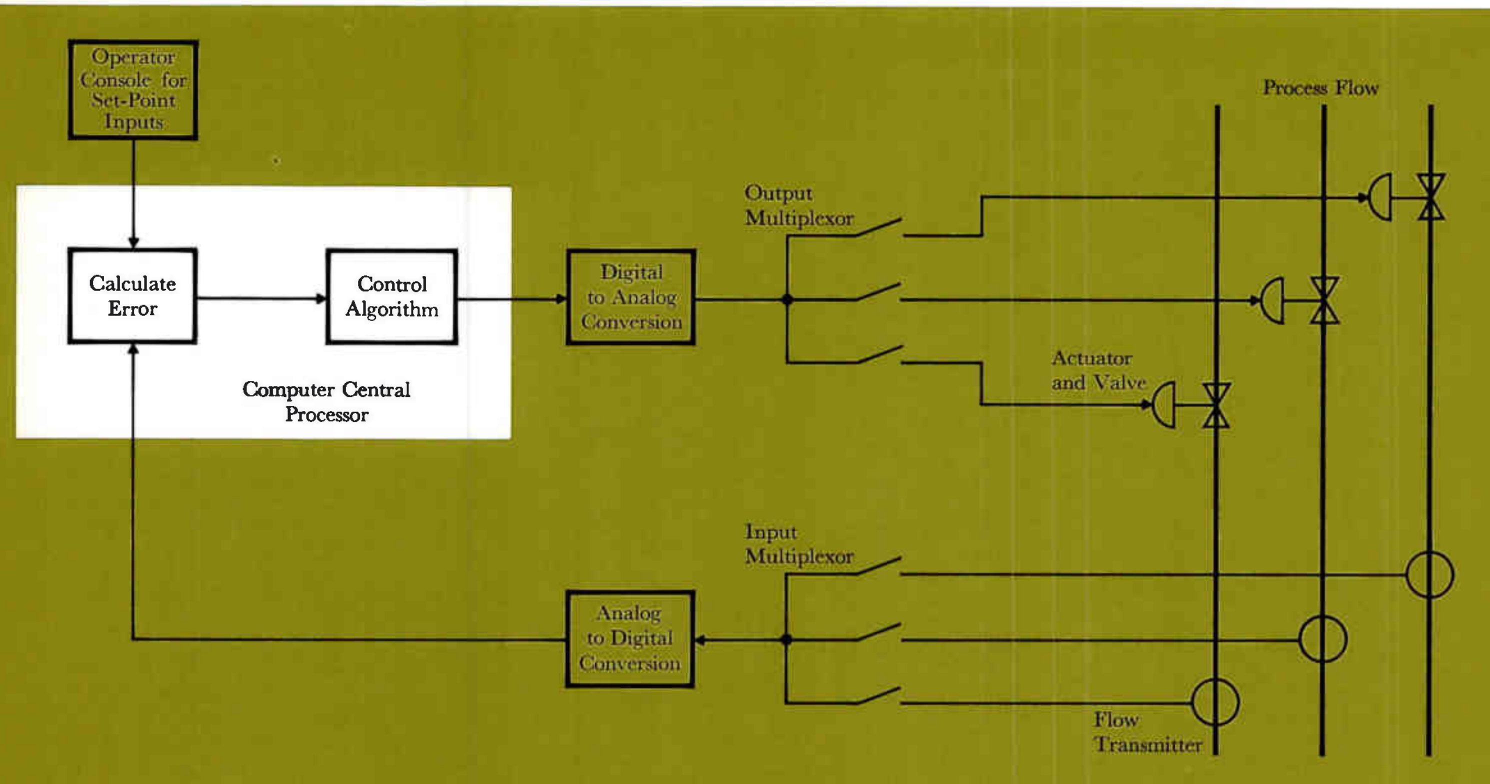

1—Direct digital control (DDC) system controls process actuators directly, rather than through an intermediate device as in set-point control. To do so, its computer makes a mathematical representation (called an algorithm) of the control equations and solves it for various process conditions. By multiplexing, as illustrated, one computer is made to control many variables in a process.

2

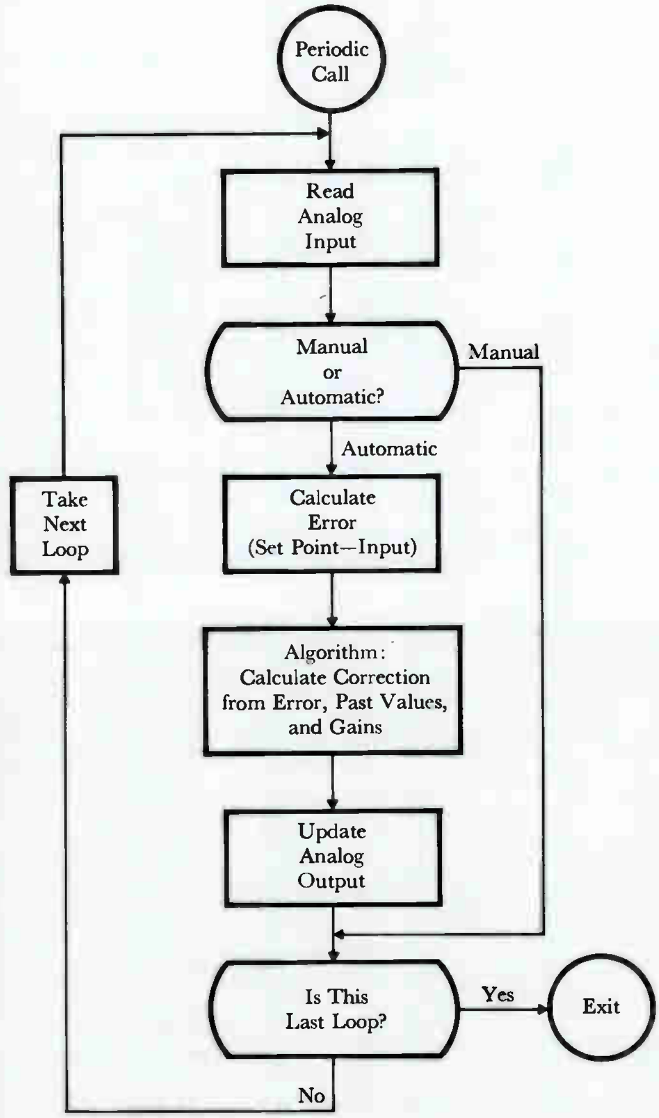

4) Loop creation. Is the ability to design arbitrary loops with arbitrary controllers desired?

5) Algorithms. What static and dynamic controllers are required?

6) Loop tuning. What set points and other parameters can be changed? By operator, process engineer, or programmer?

With the above functional specifications, tradeoffs may be necessary to arrive at a good compromise between system cost and capability, but they must be done carefully to provide a system that is convenient to use. Software organization is the key to user convenience, so several software designs are compared in the following section.

DDC Software Design

The heart of the software for DDC is the set of algorithms for each type of controller. But, while vital, that heart is often a small part of the total software. Much of the remainder is concerned with the way in which control loops are constructed and with the operator interface with the computer. The organization of the software depends on two key aspects that are common to any real-time computer problem—the data base and the timing relationship between programs. Both aspects must be considered

2—Flow chart of a basic packaged single-algorithm DDC program illustrates how the algorithm is used.

3—One of the improvements over the basic DDC system is the patchboard system. The block diagram is described by interconnection statements input to the compiler, which interprets them as control data for storage on disc. The system is flexible because of the ease of altering card input.

4—The software for the system of Fig. 3 is diagrammed here in simplified form. Much of the data comes from card input (via the compiler) and describes the control loops to be created.

5—Once the control engineer has patched his system together with the punched cards input to the compiler, the DDC director takes over. This flow chart shows how the director calls for the necessary algorithm on the basis of its periodic scans of loop data.

3

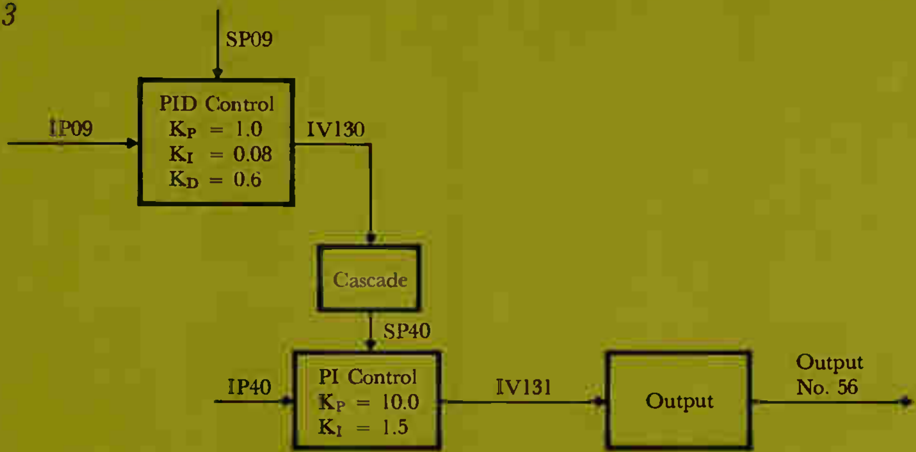


```
BGC
BGL
PID       IP09, IV130, SP09, 1.0, 0.08, 0.6
CASCADE   IV130,  SP40
EDL
BGL
PI        IP40, IV131, SP40, 10.0, 1.5
OUT       IV131, 56
EDL
EDC
```

4

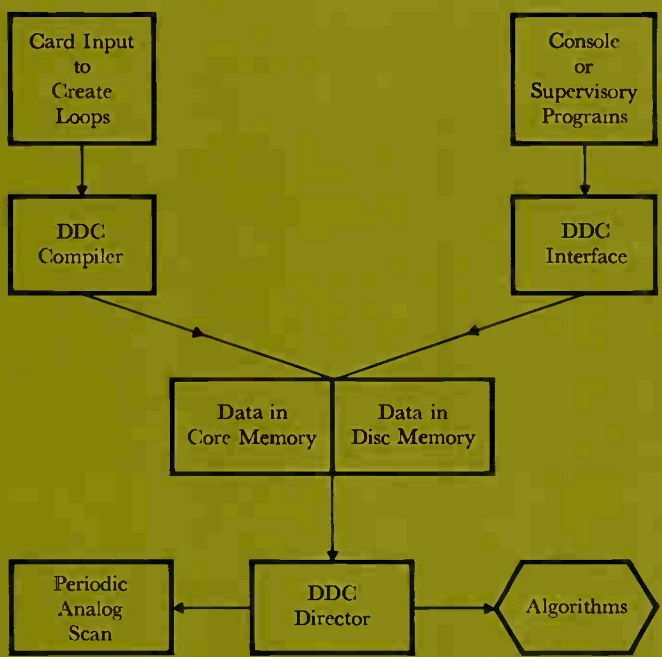

5

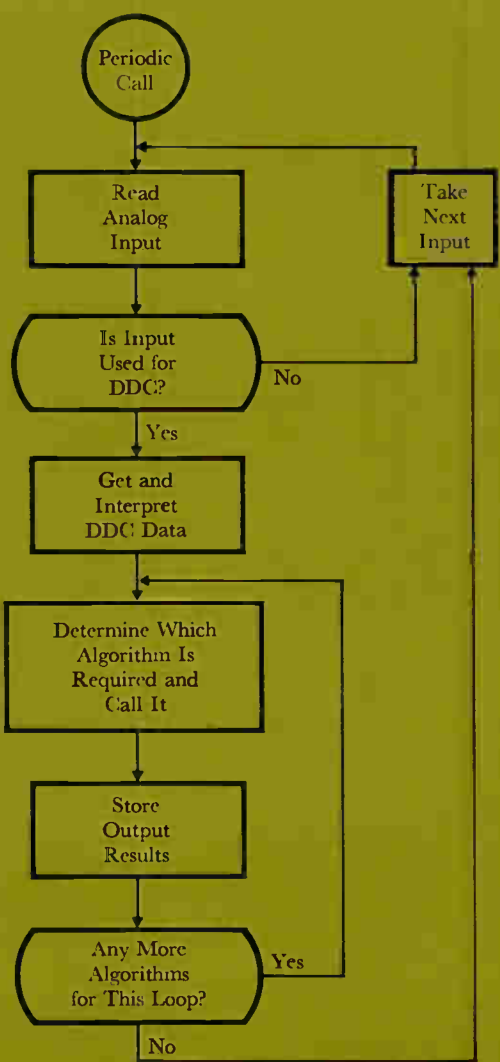

DDC Fundamentals

In direct digital control, the control action is performed by numerical calculations in the computer. The set of calculations for each type of controller is called an algorithm; some algorithms perform the same function as commonly used analog controllers, while others are unique to DDC.

As an example, consider a proportional-plus-integral (PI) controller (also called a two-mode or proportional-plus-reset controller). The output of the controller is proportional to the error (between set point and controlled variable) and to the time integral of the error. In analog controllers, various electrical and mechanical principles are used to achieve integration; in DDC, the integration is done by a numerical summation of discrete samples of the error. (The accompanying figures are graphic representations of the ideas of sampling and integration.)

Mathematically, the PI controller can be represented thus:

$$X(t)=K_P\, e(t)+K_I \int e(t)\, dt, \qquad (1)$$

where $X(t)$ is the continuous signal out of the controller, K_P and K_I are the proportional and integral control settings, and $e(t)$ is the continuous error signal. To represent the equation in a DDC algorithm, sampled variables must be used:

$$X(n)=K_P\, e(n)+K_I \Sigma\, e(n), \qquad (2)$$

where $X(n)$ is the output of the DDC controller at sample n, and $e(n)$ is the sampled error signal at sample n. For convenience in calculating controller output at any instant of time, a running sum or integral is maintained thus:

$$I(n)=I(n\text{-}1)+e(n), \qquad (3)$$

where $I(n)$ is the integral or summation term at sample n. That is, at each sample time the error is added to the summation to get a new summation. Then,

$$X(n)=K_P\, e(n)+K_I\, I(n). \qquad (4)$$

Equation 4 represents a DDC algorithm in the most simple form. While there are refinements in actual practice, the basic principles are as shown.

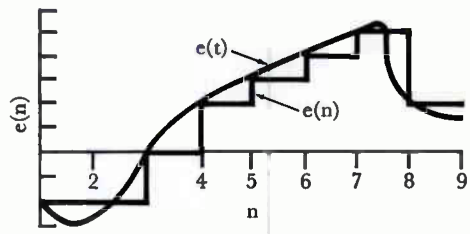

The sampled error signal takes on the value of the continuous signal at the start of each interval and holds it throughout the interval.

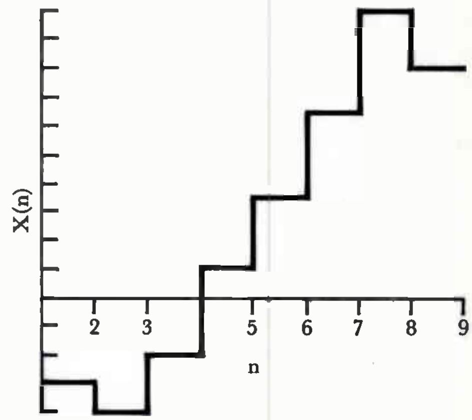

Output of the PI controller is illustrated here. The effect of the integral term is to build up the output gradually even though the input is dropping off.

In-Line Coding System

In-line coding enables the user to get the best control possible from his DDC system. In the control example diagrammed, the function generator [*f*( )] is used for a nonlinear characterization of the variable *A*. The next block (>) selects the larger of two signals, *B* or *D*. The summation subtracts this new signal, *C*, from the set point, *R*, and the resulting error goes to a proportional-plus-integral controller. Each block is represented in the in-line coding system by a Fortran statement or by a call to an algorithm. Various arrays (*BARRAY, XARRAY*, etc) are used to store such things as control constants and function generator settings.

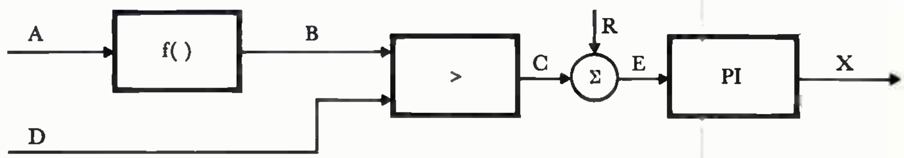


```
      CALL  FUNCT (A, B, BARRAY)
      IF B> D GO TO 10
      C = D
      GO TO 20
10    C = B
20    E = R - C
      CALL  PI (E, X, XARRAY)
      END
```

with a knowledge of the goals, constraints, and allowable tradeoffs.

Software organization concepts for DDC are illustrated by the three examples that follow. Each is representative of a class of Hagan/Computer Systems Division applications. The applications had different goals and constraints, so each accomplished its ends in a different way.

Basic System—The first example is the *packaged single-algorithm system.* It makes the most efficient use of memory and time. The conditions for its use are: small computer with limited memory; limited time per loop for DDC because of relatively slow computer, use of computer for other functions, or desire to handle as many loops as possible; each loop having fixed configuration and controlling the same basic equipment; no need to change loop configuration or sampling rate but a requirement for changes in set points and some parameters.

The data for a system of this type is organized into tables with a fixed number of entries per loop. Data for loop i, for example, is always the ith piece of data or the ith set of data in the table. Each loop has a set point, an input, and an output. Also, there are parameters corresponding to controller settings and temporary values such as the accumulation for the integral term in Equation 3 in the "box" on the facing page.

A flow chart of the DDC program is illustrated in Fig. 2, which shows the algorithm (Equation 4) and some of the associated logic. The program is called periodically to do the same calculations for each loop. This example represents, with some liberties taken, either the control of many generating units in a power system[1] or the control of many positioners in a rolling mill.

Improvements—In certain applications, users working with this basic system saw the need for improvements to realize the full potential of DDC; after all, two of the "whys" for DDC are design flexibility and control performance. Specific things users want in a software system are: usability without detailed knowledge of programming; a selection of algorithms for each loop, with ability to add new algorithms in the future; provision for arbitrary interconnection of loops; ability to add loops or change loop connections with the computer on line; and a method of performing arbitrary calculations that are not necessarily included as algorithms.

The next two organization concepts described were designed to realize some or all of those desired features. The "patchboard" system stresses flexibility with efficiency, and it can be used by a nonprogrammer. It was developed primarily for direct digital control of many linear loops in the chemical industries. The "in-line coding" system allows the Fortran-writing user to get the best possible control performance from his system. It was developed for complex and nonlinear systems such as the control of a steam power plant.[2]

The patchboard system was designed specifically to meet the user requirements mentioned previously, while keeping memory size and running time within bounds. Whereas the software for the basic system was analogous to a prewired one-to-one panel, this system gives the user the effect of a flexible patchboard. To develop a control system, he draws a block diagram and writes symbolic statements describing the interconnections (Fig. 3). The statements are punched on cards and input to the DDC compiler, a program that interprets the interconnection statements and generates data that goes into the computer memory.

The key to the system is the nature and organization of the data and the way in which it is interpreted (Fig. 4). The data in core is in tabular form very similar to that in the first example; it includes set points, inputs, outputs, and temporaries. The difference is in the loop data, which is stored on disc.

The loop data includes symbolic designation of set point, symbolic designation of input, type of algorithm (one or more), initial setting of parameters, and symbolic designation of output. This organization provides the flexibility of connecting any set point and any input to any type of algorithm available in the system. Also, the output from the controller or algorithm need not go to the computer output but can be connected to any other DDC loop in the computer.

Once the loops are created and the system put on line, another program called the DDC director scans the loop data and calls for the necessary algorithm as shown in the flow chart (Fig. 5). As a special feature, the user can specify a call to a program to do special calculations right in the middle of a loop.

The in-line coding system was developed to meet a need to perform calculations that were not part of an algorithm, a need that was of prime importance for direct digital control of a once-through boiler. It was necessary to be able to make logical decisions, make nonlinear calculations, execute an algorithm, perform more calculations, and finally output to the actuator. The system consists of in-line coding for each loop, with the code in the form of Fortran statements for logic and arithmetic and with calls to subroutines for algorithms and other functions. A typical series of expressions is shown on the facing page, *In-Line Coding System.*

Included in the system are subroutines for function generation, limiting, deadbands, and linear controllers including proportional-plus-integral (PI), proportional-plus-derivative (PD), and others. With a knowledge of Fortran, the user can construct any control system imaginable including calculations, logic, nonlinear functions, and dynamic algorithms.

Conclusion

DDC is here to stay, but the objectives and pay-off expectations have changed from mass replacement of equipment to selective use for specific problems. It is an additional control method now available and particularly suited to certain applications; as such, it supplements other control approaches rather than completely supplanting any. To achieve good results, the software system must be efficient and easy to use.

REFERENCES:

[1]C. W. Eggers and P. H. McDermott, "Methods of Digital Automatic Generation Control," *Proceedings of the American Power Conference*, Vol. 30, 1969, pp 545-550.

[2]T. Giras and R. Uram, "Digital Control Techniques for Power Plant Applications," Power Instrumentation Symposium of ISA, May 13-15, 1968, Chicago, Ill.

DC Mill Motors Rerated and Redesigned

U. M. Elder
C. J. Photiadis

Technological advances have permitted rerating mill motors to put more horsepower into a given frame size. Those same advances, plus experience and new design and manufacturing techniques, also improve motor quality.

The dc mill motor is one of the workhorses of heavy industry, employed where good speed control over a wide range, rugged durability, reliability, and fast response are prime requirements—as in steel-mill, crane, hoist, and shovel drives. The Westinghouse 600 MC motor has served successfully for 20 years in these applications and many more, but now experience, new materials, new processes, and new development techniques have relegated the 600 MC line to gradual retirement as it is replaced by the new 800 MC line of mill motors.

Such complete redesign of mill motors is an improvement opportunity for both the supplier and the user. However, redesign cannot be very frequent because many uses demand a high degree of motor standardization and interchangability. Spot improvements are made in the line as improvements in technical knowledge, materials, and processes evolve, but it is not always possible to optimize the advances without altering the established standardization or characteristics of the line. Nor can the motor characteristics be readily changed to optimize advances in such things as power supplies, processing methods, control systems, and total system designs.

The opportunity to bring out the new 800 MC motors came with the revision of the AISE Standard No. 1, *DC Mill Motor Standard*, which was completed in September 1968. Briefly, the standard established physical dimensions and mechanical and electrical characteristics recommended by a committee composed of motor manufacturers, equipment manufacturers, and users.

The most dramatic difference between the 600 MC and 800 MC mill motor is the increased horsepower rating per frame size (or volume). The rating for a given frame has been increased 20 to 50 percent over that of its 600 MC counterpart. (See Fig. 1 and table.) This rating increase was accomplished essentially by more efficient use of material and space, use of more core iron (in diameter, length, or both) on frame-size basis, improved copper-to-iron balance, and improved heat transfer.

Motor Design

At the outset of the design effort, the engineers prepared computer programs and made many runs to evaluate alternative magnetic path sizes. The results were plotted, analyzed, and optimized to size the frame, armature core, and pole areas so that total flux—main and commutating—would not saturate those parts and adversely affect either regulation or commutation.

Poles—Main poles are laminated, with eccentric pole faces to reduce armature reaction and thus give more linear torque and speed characteristics. The eccentric pole face also diminishes the main-pole influence on interpole flux, reducing the possibility of flashover at high voltages and overloads.

All interpoles are laminated and are the same length as the armature core, an improvement over the previous mill motors. (The 600 MC mill motor in smaller ratings has solid interpoles, and all sizes have poles only 80 percent of full armature core length.) Increased interpole turns, large air gaps at the armature, and brass behind each pole assure ample interpolar force to enable commutating flux to follow transient armature requirements. Use of a properly shaped pole face for correct interpole flux form plus the armature winding combination has improved steady-state commutation.

Armature—Optimizing of the armature design includes use of a large number of commutator bars with a minimum number of turns per armature coil to improve commutation by reducing reactance voltage, even though this construction is relatively costly. Reactance voltage has been further reduced by designing wide shallow armature core slots. The results are an average decrease in reactance voltage of 19 percent on a frame-rating basis, and maintenance of an average of four volts per brush at full load and base speed. (Normal design limits can be as high as 30 volts per brush.)

Some features of the 600 MC armature have been retained, such as the full-length slot wedges that give physical protection to the armature conductors in the

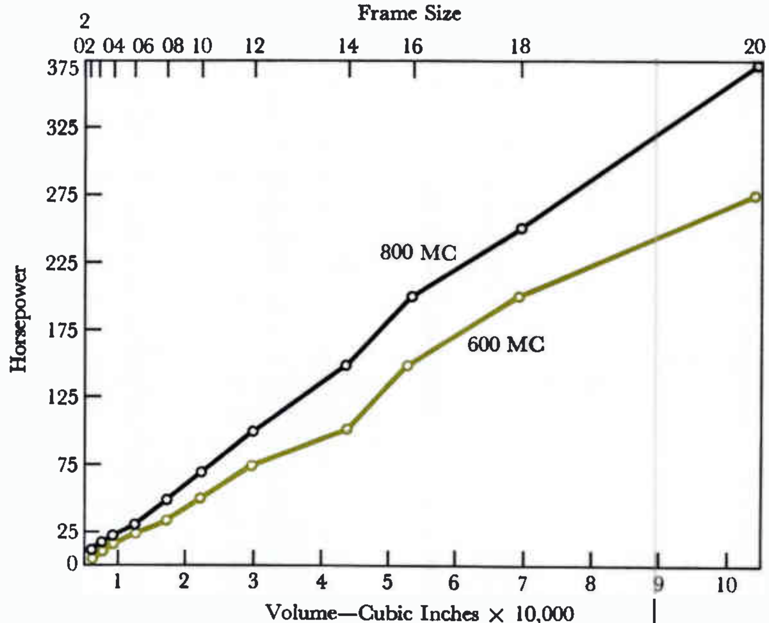

U. M. Elder is a project engineer in the Large AC/DC Motor Division, Westinghouse Electric Corporation, Buffalo, New York. C. J. Photiadis is a materials engineer there.

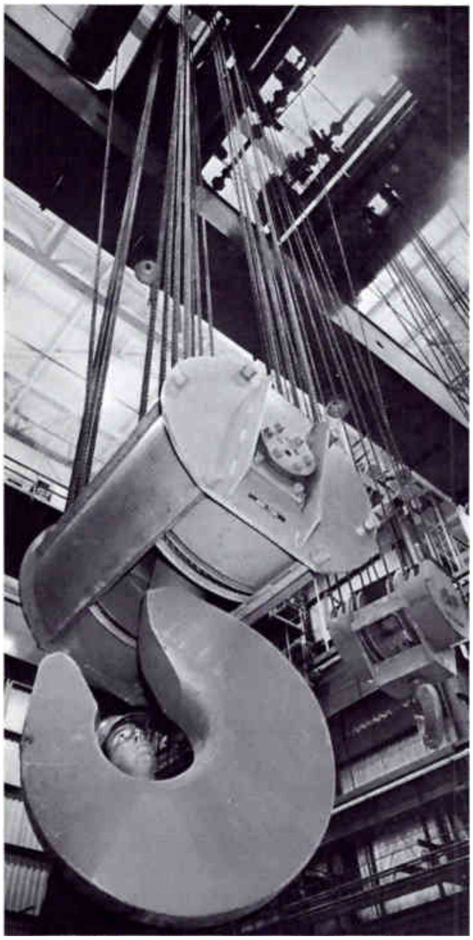

slots—in or out of the motor (Fig. 2). No fan or blower is required even with the greatly increased ratings; since there are thus no projections exceeding the core diameter, armature handling and storing are easy. The fanless cooling was achieved by use of large air ducts in the core, commutator, and winding, by improved use of the inherent air-circulating ability of the rotating armature, and by significantly improved system heat transfer characteristics.

Core and commutator are mounted directly on the large-diameter shaft with interference fits for maximum torque capability. The core is made from low-loss electrical steel laminations mechanically bound together; laminations can be replaced, if damaged, with common tools. Shaft keys align both core and commutator. A heavy cast-iron guard protects the shaft extension.

Commutator—Commutators are the conventional V-ring type for all frame sizes except 810, 814, and 818; those three are glass-banded. Glass-banded commutators have been thoroughly tested and in service for six years in industrial motors. However, because such service is not as severe as mill duty, the construction will be completely proved in service on the designated frame sizes first. That approach also will give user maintenance personnel an opportunity to become familiar with the construction on a limited basis.

The bar and mica segments in a glass-banded commutator are mounted on an insulated cylindrical steel shell. The segments are retained by resin-filled glass tape wound under high tension in grooves in the commutator surface. Retaining tension after curing exceeds the tension produced at maximum speed, keeping the bar segments from loosening.

Brush Assemblies—Commutation (the collection of current from or distribution to dc machines) is a critical link in machine performance, so the entire 800 MC current collecting system has been designed for mechanical and electrical stability in heavy-duty service. The massive gang type brush holder formerly characteristic of mill motors has been replaced by a sturdy rod and individual holder assembly (Fig. 3).

The radial type brush holder that has been so successful in motors for reversing service has been retained; it is the Conpress (constant pressure) design. It has a coil spring riding in a slip-surface saddle on top of the brush, which permits the spring to slide with brush movement and constantly exert radial pressure on the top of the brush. The brush box and integral

Comparison of Mill Motor Horsepower Ratings

Old (600 MC) Frame	HP	New (800 MC) Frame	HP	Percent Horsepower Increase
2	5	802A	5	—
—	—	802B	7½	—
602	7½	802C	10	33
603	10	803	15	50
604	15	804	20	33
606	25	806	30	20
608	35	808	50	43
610	50	810	70	40
612	75	812	100	33
614	100	814	150	50
616	150	816	200	33
618	200	818	250	25
620	275	*820	375	36

* Not included in AISE Mill Motor Standard No. 1.

Above—**Crane drives are among the applications for 800-series mill motors. The main hoist of this Whiting crane in a manufacturing plant is rated at 150 tons; it is driven by a 70-horsepower 810 MC motor. The crane's auxiliary hoist is rated at 25 tons and has a 30-horsepower 806 MC motor. Bridge and trolley drives also have 800-series motors. All of the motors are series wound and rated 250 volts dc.**

1—(*Left*) Increased horsepower rating per motor volume is the most obvious advantage of the new 800 MC dc mill motors over the 600 MC motors. Design and construction improvements make the difference and impart additional benefits. (The numbers on the top axis indicate frame sizes—2, 602-802, 604-804, etc.)

mounting support is heavy cast brass and the coil spring and retaining clip stainless steel—both noncorrosive materials to assure that the brush will not "hang up" in severe environment and service.

For frame sizes 803 and larger, the brush is a two-wafer carbon bonded at the top with a rubber pad that permits the wafers to move relative to each other and absorbs any external forces. The brush is split to increase its volts-per-brush capability; it is a proven grade of electrographitic material of high commutating ability at normal load and good commutating ability at overload.

Insulation—The AISE Standard No. 1 specifies a class B insulation system with temperature rise of 110 degrees C by resistance or 75 degrees C by thermometer—essentially the same as for the 600 line of motors. Insulation and heating considerations go together in the design of the 800 MC, because ability to increase ratings from 20 to 50 percent is primarily proportional to the ability to transfer heat from heat-generating areas to the outside air.

The 800 MC is a class F motor with class H materials in areas of heat concentration. This higher class insulation system provides the user with a motor that has longer life when operated under normal rated loads, has the ability to remain in operation under many severe

2

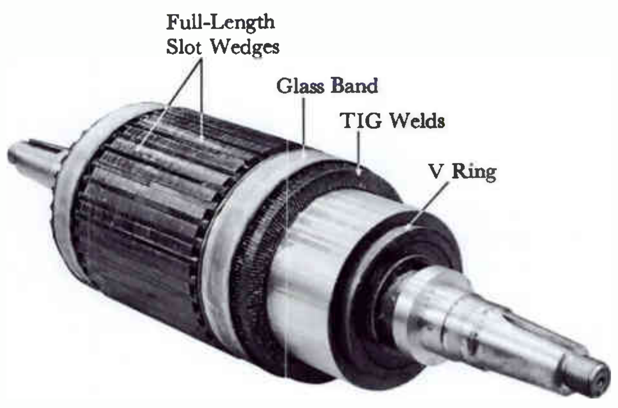

3

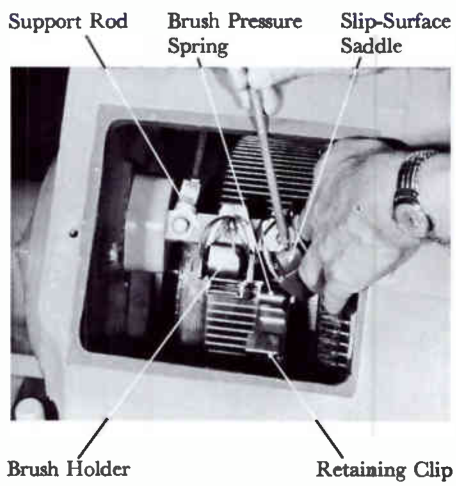

4

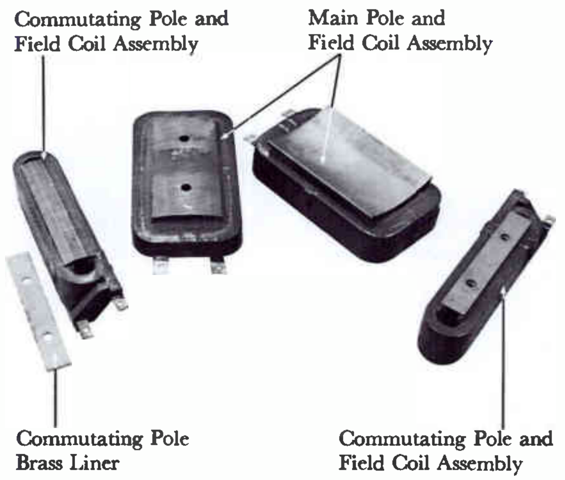

5

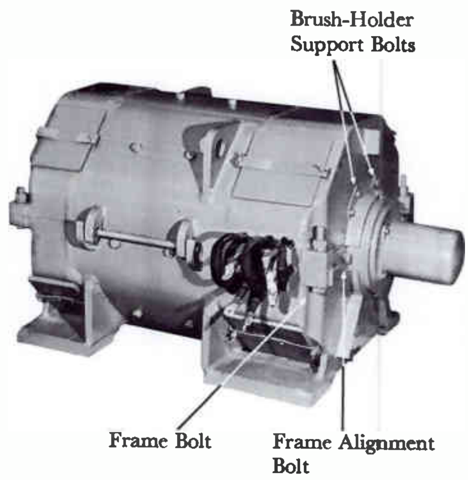

overload conditions where a standard class B system would fail, and is capable of continued operation in severe peak load applications that would degrade a class B insulation system even though rms loading would dictate the lesser insulation level.

Armature coil conductors are covered with a high-temperature insulation proven in service by our industrial, mining, and special 600 MC motors. Each coil in the core slot is tightly wrapped with a high-temperature high-dielectric combination, providing maximum insulation between coil sides and from coil sides to ground. The coil wrapper ends are sealed well into the coil crossovers to exclude contaminants and to increase creepage distance to ground. Each coil is then inserted into a slot liner to protect it from damage when winding. This system makes a highly compacted assembly that assures maximum heat transfer from coil to core iron. Coil extension insulation is reinforced at stress points.

The area immediately behind the commutator risers is completely sealed from carbon dust and other conducting materials to eliminate the possibility of establishing a creepage path to ground. Equalizing connections used in the larger frame sizes are made from the same type of conductors as the armature coils, individually insulated and compactly sealed behind the commutator risers.

2—Armature end turns are secured with glass-fiber tape banding. Coils and equalizer connections are TIG welded to the commutator.

3—Commutator access opening is large to facilitate adjustments and maintenance. Here a brush holder and rod assembly is seen through the opening.

4—Field coils are encapsulated and then potted onto the poles. The result is a sealed unit with excellent heat-transfer properties.

5—All but the largest sizes have hinged upper frames secured by a bolt at each corner, as in this 812 MC motor. Covers that require periodic removal for inspection and service have thumb screws for easy removal. Leads are brought out individually. The motor shown is a series-wound totally enclosed nonventilated unit rated 100 hp, 230 volts, 475 r/min, one hour 75-degree-C rise.

The armature coils are compacted and rigidly held in the core slots by high-temperature wedges extending the full length of the core (Fig. 2). End turns are glass banded, with tensions that exceed the operating loads, to prevent any movement.

After armature coils and equalizer connections are TIG welded to the commutator, the armature is vacuum impregnated in a high-temperature varnish. The result is a system with maximum heat transfer characteristics and maximum resistance to contamination.

An obvious change to users familiar with the 600 MC motor is in the field coils—their exotic green color and their encapsulated potted-on-the-pole construction (Fig. 4). Coils that are wound from round or rectangular conductors have the conductors coated with a high-temperature enamel and are treated with a high-temperature bonding agent. With the winding firmly compacted and restrained, the bonding agent is thoroughly cured to produce a rigid self-supporting coil. The coil has maximum turn-to-turn contact and filled interstices for excellent heat transfer. It is then encapsulated in a special resin to completely seal it from contamination.

This coil insulation system is the result of an extensive materials and manufacturing development program undertaken to obtain in-place coating with excellent bond strength to the substrata, uniform build, freedom from pinholes, required thickness, mechanical soundness, and thermal shock resistance.

The encapsulated coil is bonded to the pole with a potting compound specially developed for excellent bond strength and heat transfer, low shrinkage, a coefficient of expansion approaching that of metal, and high-temperature thermal endurance. The manufacturing process applies the compound properly and completely so as to make a completely unitized coil-and-pole assembly. The assembly is a mechanically stable system with a sealed winding that is designed for reliability and has excellent heat transfer characteristics—at least twice the heat transfer capability of the 600 MC assembly of steel shell and coil.

Bare-strap coils are bonded together with a high-temperature resin-bonded inorganic paper. The coils are then encapsulated and bonded to the poles in the manner just described.

Connections—All internal joints are insulated to seal the connections and eliminate creepage failure there. Lead cables and cross-connecting cables are brought out through individual rubber grommets, insuring positive electrical and mechanical protection and spacing (Fig. 5).

Performance

Increasing the horsepower of each frame size has decreased the floor area per horsepower by an average of 15 percent. Judicious design has held the increase in weight per frame size to an average of only 6 percent, and decreased weight per horsepower by an average of 19 percent, while keeping the motors compliant with the AISE Standard (Fig. 6).

All this is in keeping with the trend to better and smaller equipment. It is especially significant in, to name but a few examples, new mills where large numbers of motors are used, electrical shovels where space is at a premium, and cranes where weight is critical. Moreover, equipment builders' design problems are decreased by smaller and lighter motors. In short, the reduction in size per horsepower increases the ultimate economic advantage to the user.

Mill motors are generally applied to drives requiring a high initial torque. Torque per frame size is established by the AISE Standard; it is an average of 36 percent higher in 800 MC motors than in 600 MC motors (Fig. 7). Torque per ampere, based on horsepower rating, is on the average 10 percent greater in the 600 MC motors than in the 800 MC. The difference is the result of retaining the same speed for the given frame size.

Armature inertia (based on horsepower rating) is reduced by the more efficient use of materials inherent in the new developments applied. Only a portion of the 600 MC inertia is encountered when accelerating an 800 MC motor of the same rating; or, for a given power input to accelerate to the same speed, the rotational response is faster.

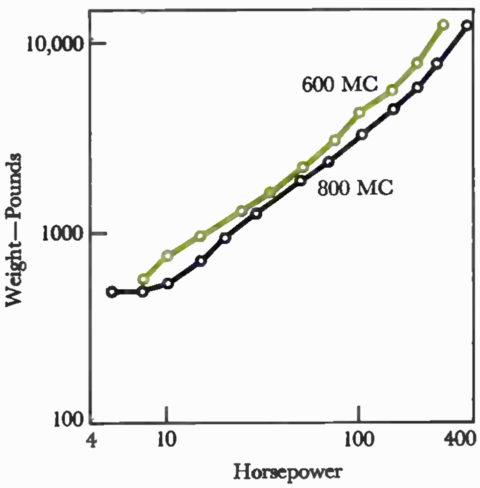

6—Weight per horsepower has been decreased an average of 19 percent while increasing horsepower per frame size 20 to 50 percent.

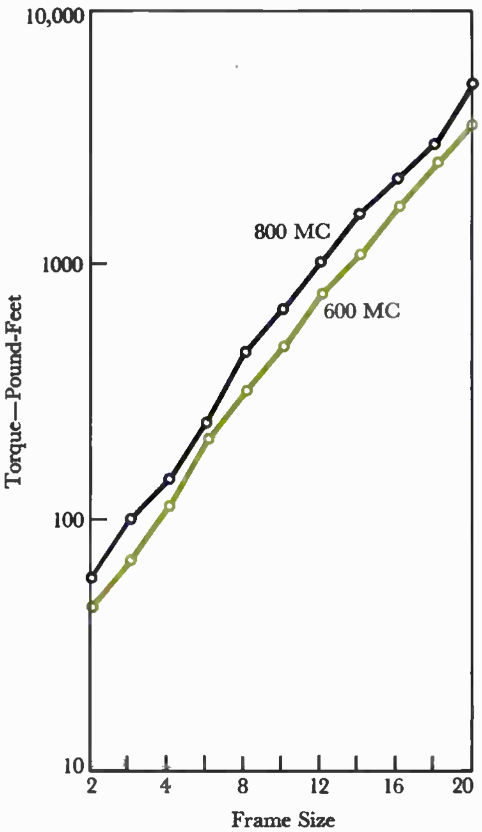

7—Torque per frame size averages 36 percent higher in 800 MC motors than in 600 MC motors; it is established by the AISE Standard.

Construction and Maintenance

Standardization of the bottom openings used for forced ventilation from an external source has increased the versatility of 800 MC motors, permitting mechanical interchangability of motors of all suppliers. It should not be taken for granted, however, that these motors are interchangable electrically in a given drive system. Nominally, series and compound motors may be used interchangably.

The frame is all-steel split construction with through bolts clamping the halves together at the four corners. Hinges with lugs permit the top half to be opened 90 degrees without external support on frames 802 through 812, and the hinge pins can be removed for complete separation of frame halves. The 814 and larger motors do not have hinges, so the top half must be removed for major servicing.

Assembly and disassembly are much the same as with the 600 MC motors. Opening is the same, but armature removal requires only disengagement of four frame alignment bolts (two at each end) from the bearing cartridge flanges.

Commutator access openings were made as large as possible for ease of inspecting and servicing the brush rigging. The entire commutator end, in fact, was designed to limit down time, facilitate servicing, and reduce maintenance costs. The brush holder rod assembly is mounted with two external bolts—accessible from the front of the motor—without resorting to tapped holes or welded mounting supports in the frame. Each rod can be removed and replaced accurately and rapidly with simple tools and without disassembly of the motor.

Individual brush boxes can be replaced, in contrast to the more costly gang type holders of previous designs. Seven brush holders and brushes serve the entire 800 line—a 32 percent reduction in inventory requirements.

All armature conductors are TIG welded to the commutator risers for reliable mechanical and electrical joints that keep the motor operating through overload situations that would normally fail solder connections. If rewinding is required, the TIG joints can easily be machined off, leads lifted, and rewinding performed. The new conductors can be joined to the commutator by TIG welding or by soldering, depending on facilities available. Commutators can be repaired in the field also.

Bearings are the roller type specified by the AISE Standard. The bearing assembly, clamped between top and bottom frame halves, is removable for quick and easy inspection. Greasing has been improved by decreasing the length and increasing the diameter of the drain passage, thus reducing the amount of pressure required to force grease into the assembly and minimizing the possibility of overgreasing or forcing grease into the motor.

The unitized pole and coil assembly follows the trend of using subassemblies for one-piece replacement, which reduces the number of pieces needed as spares. In an emergency, the assembly can be repaired: a failed coil can be removed by heating and pressing off, and the pole can then be cleaned and a new encapsulated coil repotted on it. In an extreme emergency, a conventional taped coil could be mounted on the pole, properly restrained, and operated (at increased temperature and loss of efficiency) until the correct repair or replacement could be made.

Frame openings are provided so that all conventional enclosures can be formed by mounting appropriate covers. No machining is required to change the type of enclosure from the nominally standard totally enclosed nonventilated configuration to open protected (self ventilated) or to totally enclosed force ventilated from an external source or from a motor-mounted blower. It is necessary, however, to remove the armature to install the shaft-mounted blower for the self ventilated enclosure. No machining is necessary to add standard appendages such as tachometers and overspeed devices.

Conclusion

The 800 MC motor is a new motor designed to the expressed requirements of users. It incorporates the advances of the past 20 years in materials, techniques, and processes to surpass the enviable record established by all preceding mill type motors.

Improved Digital Simulation for Analyzing Power System Disturbances

C. J. Baldwin
R. T. Byerly

A new digital computer program that incorporates recent advances in power systems analysis techniques provides a powerful tool for studying system stability following a fault or loss of generation, transmission, or load.

Utilities have built extensive EHV transmission systems and substantially increased unit ratings in recent years. The requirement for high reliability of these systems has led to the development of improved methods for analyzing system dynamics following major disturbances. One measure of system security is stability following a fault or loss of generation, transmission, or load. Stability can be effectively evaluated by a new digital computer program developed by Westinghouse. A system simulation with this new program can accommodate as many as 2000 buses, 3000 lines, and 600 generating units. Systems with as many as 100 generating plants have been studied.

Generator units are represented in detail with mathematical models that include variable internal machine voltages, the effects of faster-acting automatic excitation and governor systems, and prime-mover torque variations. Bus frequency deviations are computed, and load-shedding studies are possible. Two hundred relay locations can be simulated with automatic line switching and reclosing. Dc transmission lines can be included in the simulation, and real and reactive power flows at the converter terminals can be computed. The increased size and detail of the new system simulation program is made possible by the availability of new large-memory digital computers.

Approach to Dynamic Simulation

Since machine acceleration results primarily from positive-sequence torques, only the positive-sequence network is represented in the system simulation. However, the effects of unbalanced faults on positive-sequence torques can be included by using appropriate symmetrical component fault impedances.

The dynamic simulation proceeds stepwise with two alternating stages of calculation. The first is a load-balance stage, in which time is invariant. It occurs every 10 to 20 milliseconds of real time for the system. During each load balance, an iterative load-flow technique determines bus voltages and line flows for specific generator internal voltages, transmission impedances, and load characteristics. Changes in the transmission system due to predetermined switching conditions or relay operations are made in this stage, and load shedding may occur. Load balances are made before and after all line switching and for the application and removal of faults. Checks for conditions that require load shedding are made after each load balance. If load dropping is indicated, it will occur at the succeeding load-balance calculation.

In the interval between load balance calculations, time is variable and each generator is coupled to the system through terminal voltage extrapolation. Generator rotor velocity, position, and internal voltage change with time are determined by differential equations. The same is true of governor and excitation system time-dependent variables. During each dynamic interval prior to the next load balance, generator terminal voltages are assumed to change by simple extrapolation of their recent history if switching has not just occurred. If switching has occurred, extrapolation is not applicable due to discontinuities, and, for a brief period, terminal voltages are held at their most recently determined values.

By using a time-variant dynamic interval between load balance stages, integration step size for each generator can be independent of the load balance interval and independent of integration step sizes for other generators. Thus, the integration step size for each generator can be kept consistent with the smallest time constant in the generator, governor, or excitation system.

Synchronous Machine Representation

The equations that represent synchronous machines fall into three categories:

1) *Swing equations* govern the relative velocity and position of each machine rotor.

2) *Internal voltage equations* are variable in number, and they depend on the type of generator and the detail of its representation. Up to six first-order differential equations may be involved, four related to the quadrature-axis voltage and two related to the direct-axis voltage. The equations provide complete representation for steam turbine generators, waterwheel generators with continuous damper windings, and waterwheel generators with discontinuous damper windings. The program selects the most complete representation possible for the input data provided, and checks the consistency of input data for that representation.

3) *Coupling equations* couple the real and imaginary components of internal generator voltage to the real and imaginary components of terminal voltages. If voltage behind subtransient reactance is being computed, the subtransient reactance couples the internal voltage to the terminal voltage. If the voltage behind transient reactance is computed, transient reactance constitutes the coupling to the terminal voltage.

The performance of a completely represented steam turbine generator during a 15-cycle three-phase fault at the high side of the unit transformer is shown in Fig. 1. The machine is rated at about 600 MVA, and peak short-circuit current is somewhat over 3 per unit on the machine base. The generator excitation system and turbine governor are also simulated, which accounts for the variations in field voltage and turbine torque. These curves were taken from a study that included more than a hundred generating plants or equivalents in varying detail.

Excitation Systems

Excitation systems are of interest in stability analyses because of their influence on critical clearing time and on the damping of rotor swing angle oscillations.

The general effect of the excitation system is to reduce the initial rotor swing

C. J. Baldwin is Manager of Development, Advanced Systems Technology, and R. T. Byerly is Advisory Engineer, Development, Advanced Systems Technology, Power Systems Planning, Westinghouse Electric Corporation, East Pittsburgh, Pennsylvania.

angle by increasing the flux level in the machine during periods of low terminal voltage. Increased flux causes a greater restoring torque, which slows the machine more rapidly after the fault clears. Thus, an excitation system with a high exciter ceiling and a high speed of response to reach this ceiling will minimize the first swing. However, this action does not necessarily improve dynamic conditions following the first swing and, in fact, may often contribute negative damping.

Modern excitation systems are manufactured in many forms, but most of them can be represented by one of several general mathematical models. Three of these general models are described in the diagrams in Fig. 2.

The limitation on the minimum time constant for excitation system simulation has been set at 0.02 second. Smaller time constants require smaller integration step sizes, and their effects generally do not alter results significantly because they occur in cascade with larger time constants, and the natural frequencies of the electromechanical system are low in comparison.

In general, the voltage damping feedback loops are simulated without mathematical elimination. The existence of a damping loop results in effective excitation system time constants which are not apparent from normally available system parameters. For most conventional excitation systems, the closed loop time constants are large enough to be simulated. However, for very fast systems that employ damping feedback, the closed loop time constants may be very small. Adjustment of integration step size to accommodate such small delays would be unnecessarily expensive. Therefore, if very small step sizes are required, calculation is terminated following the initial part of the program, which is devoted largely to data diagnostics. An error message pinpointing the problem is printed.

To handle very fast exciters, a special system that cannot have exciter saturation and consequently cannot have self excitation is permitted in the simulation. The input routines recognize this very fast excitation system as one in which mathematical elimination of feedback is possible.

Voltage Regulator Auxiliary Input Functions

Auxiliary signals can be applied to voltage regulators to improve the damping of rotor oscillations. To illustrate improved damping, the performance curves of a waterwheel generator, taken from a system study, are shown in Fig. 3. These curves show the inherent damping of the generator without governor or voltage regulator (Fig. 3a), the unstable behavior with governor and voltage regulator (Fig. 3b), and the improved damping obtained by feeding an accelerating power damping signal into the voltage regulator (Fig. 3c). The machine being simulated exhibits these characteristics quite closely in field tests.

Damping action of the excitation system may be improved by sensing any of several variables other than voltage error, filtering the signal to obtain desired phase relationships, and then adding it to the normal voltage error. To accommodate the various possibilities, the computer program permits voltage regulators to have an auxiliary input from any two of the following signal sources: machine slip, accelerating power, electrical power, terminal voltage deviation, or bus frequency deviation.

Governors and Energy Systems

When operating under normal system conditions, machine governors do not exhibit strong responses to changing system loads. System frequency remains relatively constant, with excursions from 60 Hz limited to about ± 0.01 Hz. The dead band of mechanical governors prevents any significant speed regulation for such small speed errors.

Machine power changes under such slowly changing conditions are usually made under the direction of the load-frequency control system. Raise and

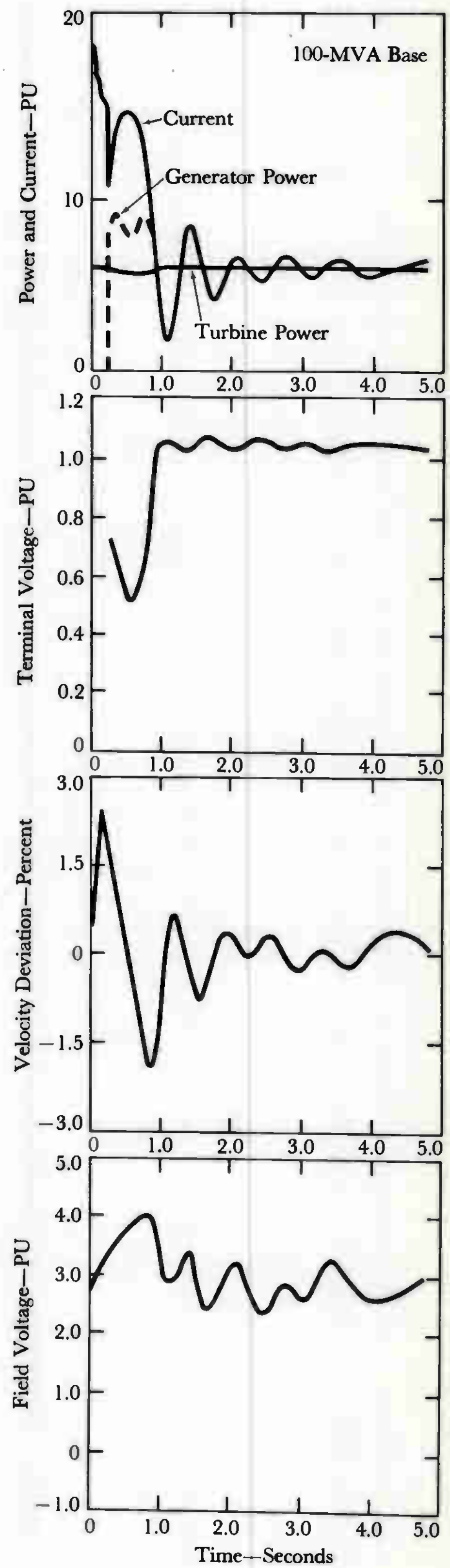

1—Generator performance is illustrated for a 15-cycle three-phase fault at the high side of the unit transformer.

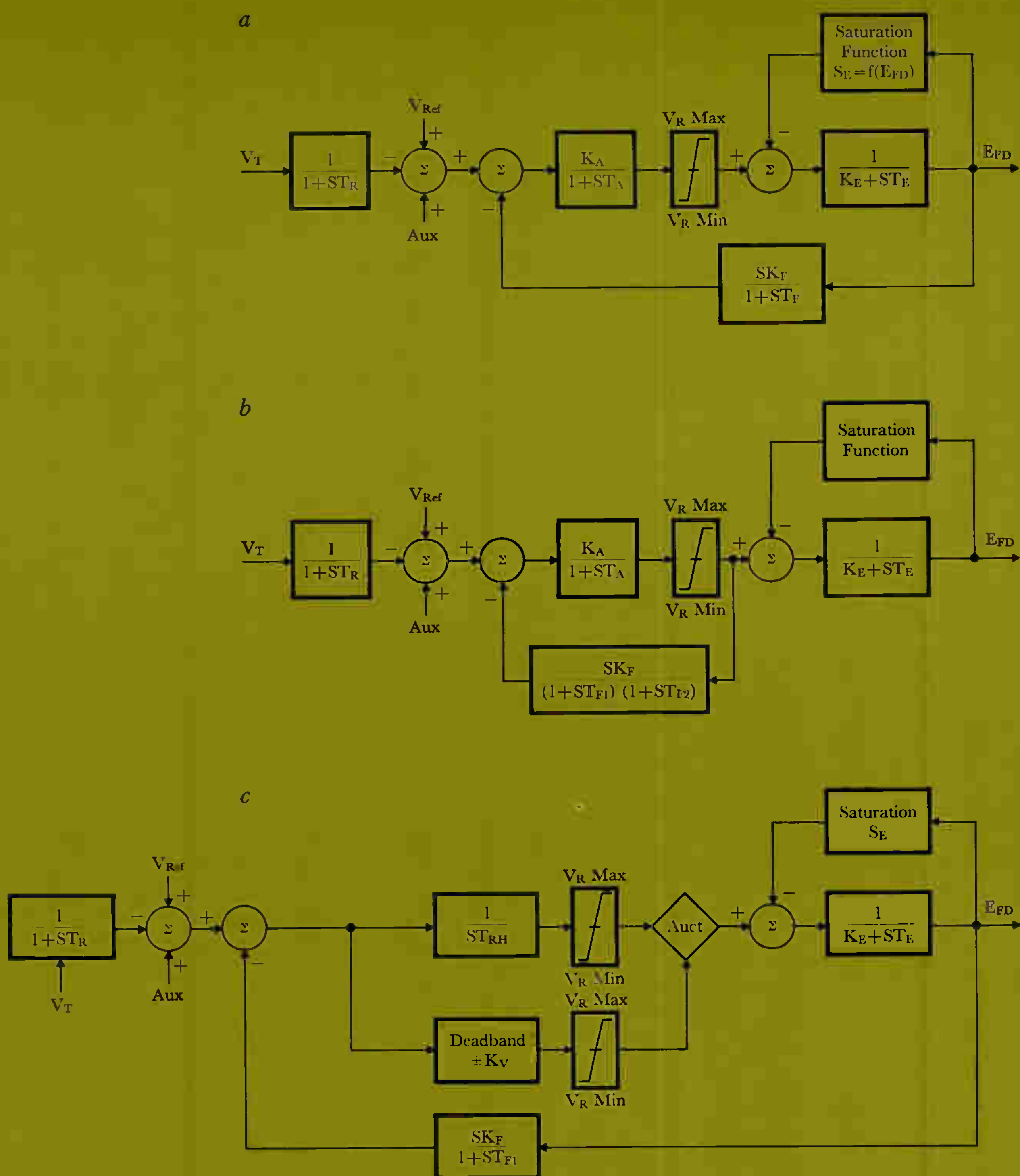

2–Block diagrams of frequently encountered excitation systems. Two configurations of continuously acting regulators and either ac or dc exciters are shown in (*a*) and (*b*); a noncontinuously acting regulator and a dc exciter are represented in (*c*).

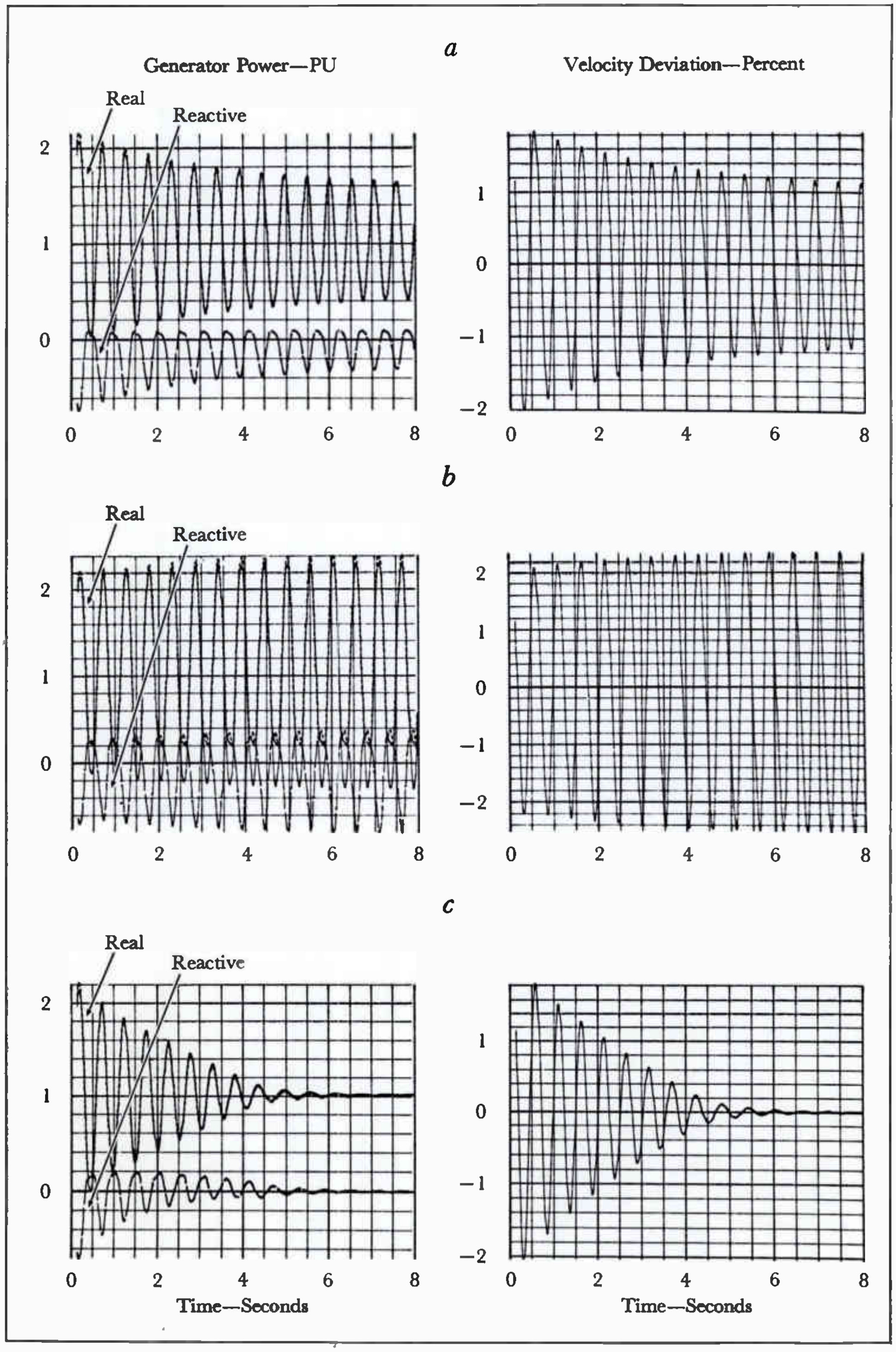

3—Damping characteristics of a waterwheel generator are illustrated by these performance curves: (*a*) with no governor or voltage regulator action simulated, (*b*) with governor and voltage regulator action simulated, and (*c*) with governor and voltage regulator simulated and with a special damping signal acting through the excitation system.

lower pulses change the setting of the speed governor, and machine output power adjusts so that operation is again at the point on the governor load-speed curve corresponding to the system operating frequency.

The newer electrohydraulic governors provide closer machine load control by paralleling the normal speed governor with a load controller. The speed reference, speed droop, and load reference may be set independently. Machine response is primarily to the load reference but added to any speed error based upon a 5- to 8-percent speed droop.

The representation that is generally used in digital computer simulation includes only the speed-governing system. The block diagram used in the Westinghouse program is shown in Fig. 4.

When the system is subjected to a severe disturbance, such as an electrical fault, the load-generation balance is upset and accelerating and decelerating powers are impressed upon the various machine inertias. Since rotor speed cannot change instantaneously, there is little speed-governor response for the first half second. If the fault is cleared quickly and the system is electrically stable, the oscillations normally damp out with only a small speed-governor action. For fast oscillations and a study time of one or two seconds, no governor action and constant mechanical input power to the unit usually can be assumed. However, for longer study times the influence of speed-governor and prime-mover energy systems may be important.

This is especially true in an investigation of several seconds duration where damping of sustained oscillations is being investigated. In these cases, speed-governor action may significantly alter system response.

Speed governors for hydro-generators can have a major effect on generator response because of the inherent negative damping of the water column. To illustrate the effect of water inertia, consider the velocity and turbine power curves shown in Fig. 5. The machine is part of a large system, and the fault that produces the initial disturbance is relatively remote. But note the phase relationship between velocity deviation and turbine power. Even though the initial velocity is increased, turbine power does not initially decrease. The effect is one of negative damping with peak velocity deviation occurring after the first swing. This illustrates the importance of correct representation of hydro-governors in a system study carried beyond the first swing.

Fast Valving for Steam Turbines

The modern electrohydraulic turbine governing system has the ability to rapidly close the intercept valves upon detection of high accelerating power. This feature can be used to improve transient stability (or reduce the first swing peak angle). The computer simulation detects the drop of generator output power below an input criterion, caused by a severe fault or opening of the generator breaker, and initiates a linear closing of the intercept valves after a specified time delay. When the fault is cleared, power recovers to near normal, and valve opening is simulated by a linear ramp at a slower rate.

Simulated fast valving action is shown in Fig. 6. Two units in a two-unit plant experience an eight-cycle, three-phase high-side fault (Fig. 6a) and are stable after a severe swing. Note that there is only a minor response from the speed governors. In Fig. 6b, one of the two machines (unit 1) has fast valving, which initiates interceptor valve closing. The maximum angle swing of unit 1 is significantly reduced, and unit 2 is somewhat lower.

Studies have indicated that critical clearing time can be improved by approximately one cycle with fast valving on one unit and by about two cycles with fast valving on both units.

Relay Representation

Power swings subsequent to a disturbance may cause relays to operate and breakers to trip. Earlier computer programs required the user to provide tripping times as input data for all switching conditions. If cascaded line trippings were to be simulated, repeated analyses of results were required to determine which relays had entered trip zones and when breaker operation would have occurred. This was followed by repeated runs with the switching represented. This technique proved to be prohibitively expensive and time consuming. To overcome this problem, provision has been made for the simulation of impedance, over-current, out-of-step blocking, and overpower relay functions at up to 200 locations in the system. These relaying functions are intended for use primarily during swings when the positive-sequence simulation is assumed to represent real network conditions. The ability to input switching sequences associated with fault clearing has been retained.

The impedance relay is characterized by three circles in the R-X plane. Each circle represents a zone of protection and is represented by a radius and center. At each load balance the program calculates the apparent impedance of each relayed line from its positive-sequence voltage and current. When apparent impedance enters one of the zones, a timer is simulated to record the time spent in that zone. If the timer reaches the preset maximum time for the zone, breaker operation is initiated, and the breaker is tripped after enough additional time has passed to account for the time required for breaker operation.

The amount of time from the line opening until the breaker is reclosed can also be specified. If the apparent impedance moves out of any zone before the trip time has elapsed, the program assumes an instantaneous reset. An additional option allows the program to simulate directional elements by specify-

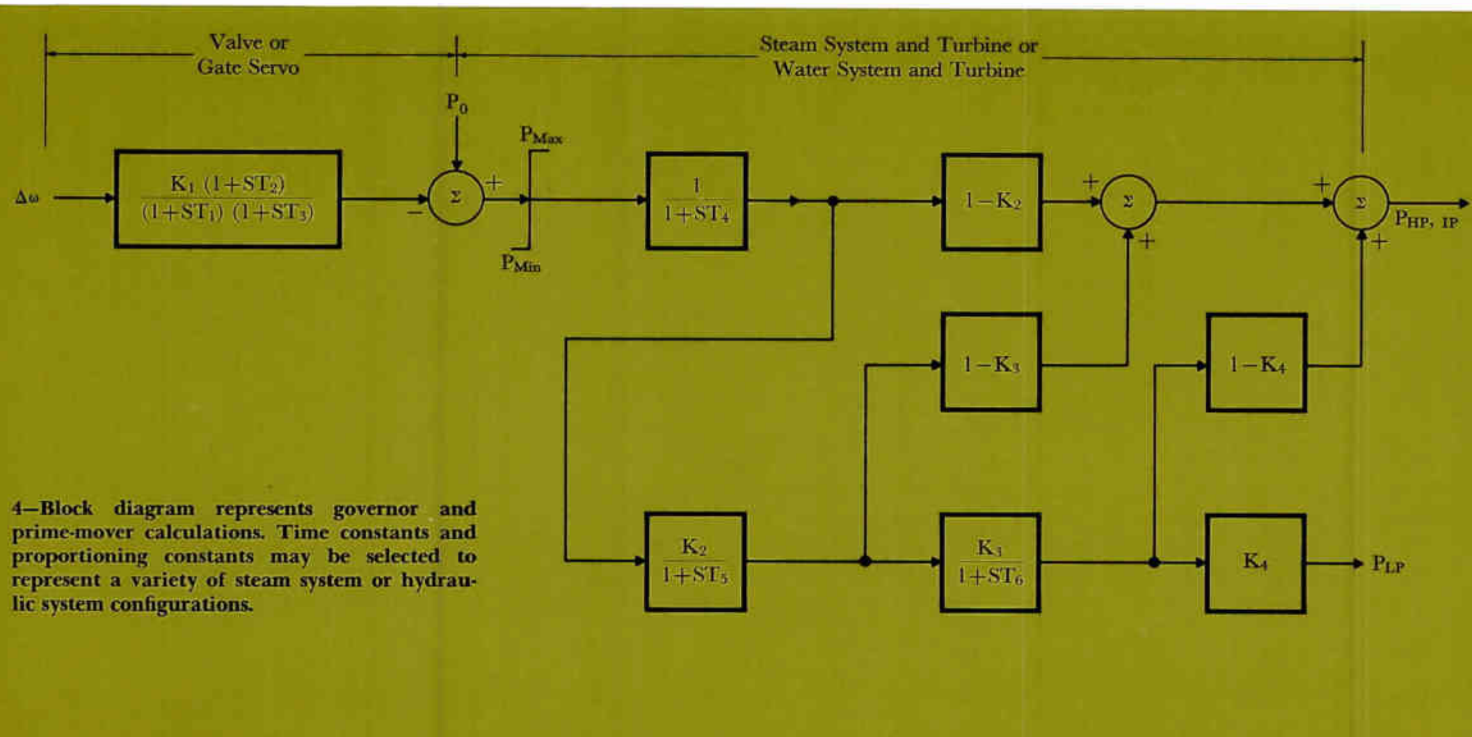

4—Block diagram represents governor and prime-mover calculations. Time constants and proportioning constants may be selected to represent a variety of steam system or hydraulic system configurations.

ing that a portion of the R-X **plane is** outside the impedance zones.

The program also provides for the representation of out-of-step blocking relays. The relay is characterized much the same as the impedance relay. Again, three zones are represented, but only two are trip zones. When the apparent impedance enters the outside zone, breaker operation is blocked if the timer of that zone reaches the preset maximum before the impedance enters the next zone. This feature prevents breaker operation for slow power swings while maintaining protection against abrupt power changes.

The specification and use of overcurrent relays has been greatly simplified by storing in the program the characteristics of the most commonly used relays. The program makes use of routines developed for a relay coordination program to calculate the time required for the relay contacts to close for various values of current.

The ability to simulate overpower relays is also provided. The representation and contact closing calculation is the same as that of the overcurrent relay. Line power is monitored instead of current, and time for the relay contacts to close is a function of power.

To provide additional versatility, logic has been included to allow the combination of two or three impedance type relays to control a breaker operation. These relays can be at the same location, or they can be on different lines. Carrier functions can be simulated by making the breaker operation dependent on the apparent impedance being in a given zone at all the controlling locations.

DC Line Representation

Three two-terminal, two-pole dc lines can be represented. The assumption is made that two operating modes are possible. In mode one, the rectifier regulates current by adjusting the rectifier firing angle, and the inverter maintains a constant angle of extinction. In mode two, the rectifier operates at zero firing angle, and the inverter regulates current.

The program tries to operate the line in mode one, but changes to mode two if the rectifier voltage is too low for mode one operation. No converter transformer tap adjustments are made during a stability study. The objective in stability calculations is to properly simulate power and var flows for slowly changing system conditions. The models used are not intended for detailed studies of dc lines for ac system faults near the converter terminals.

Automatic Load Shedding

Loads are usually sensitive to voltage magnitude and frequency, whether they are assumed to be motors or general loads. Voltage magnitudes at buses are computed as transients, and load sensitivity to voltage is normally considered in present-day stability studies. Sensitivity to frequency has only recently been taken into account because of interest in load shedding and the effects of load on the damping of power oscillations.

The new dynamic stability program allows load shedding to be based on either voltage magnitude or frequency deviations at any of the 2000 buses represented. The calculation of a transient frequency at each bus is required. This stems from the fact that magnitudes and time phases of frequency deviations are not the same at all buses any more than are generator rotor speeds. The latter are, of course, integrals of rotor accelerations, and there is no question of their availability or reliability within the general assumptions pertaining to stability studies.

Bus frequencies are not so readily available. Rotor speed deviation from normal speed can be obtained at least approximately by differentiating rotor phase angles, and this suggests that approximate bus frequencies can be obtained by differentiating bus phase angle functions. Carrying out this calculation in the program requires saving past values of bus angles and using an approximate differentiating formula.

Typically, automatic load shedding is based on underfrequency conditions and occurs in several steps. If the initial load dropped does not halt the drop in frequency, the second step of load shedding occurs and, of course, may be followed by successive steps. Three steps of load

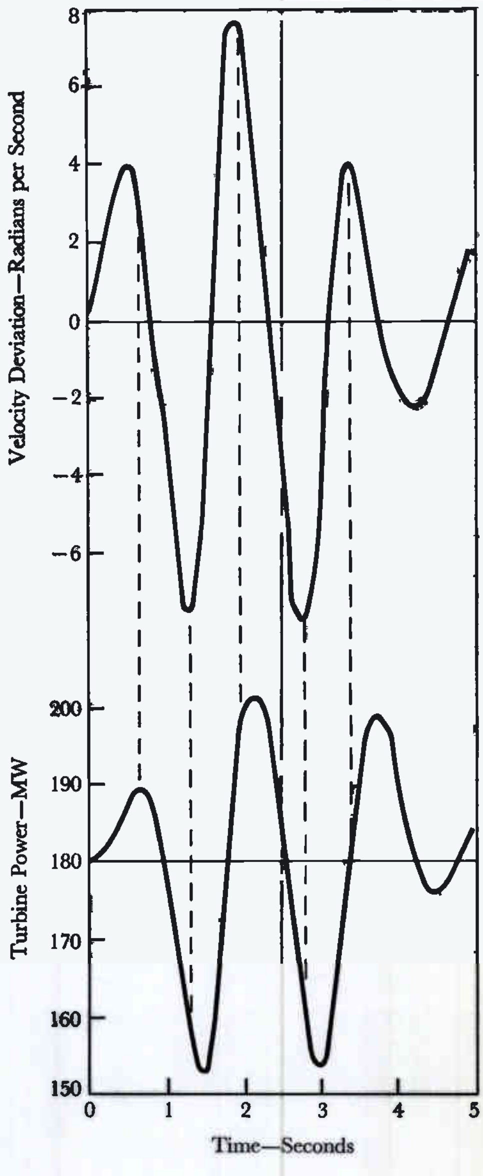

5—Response of a waterwheel generator to a remote disturbance, emphasizing the effect of water inertia on damping.

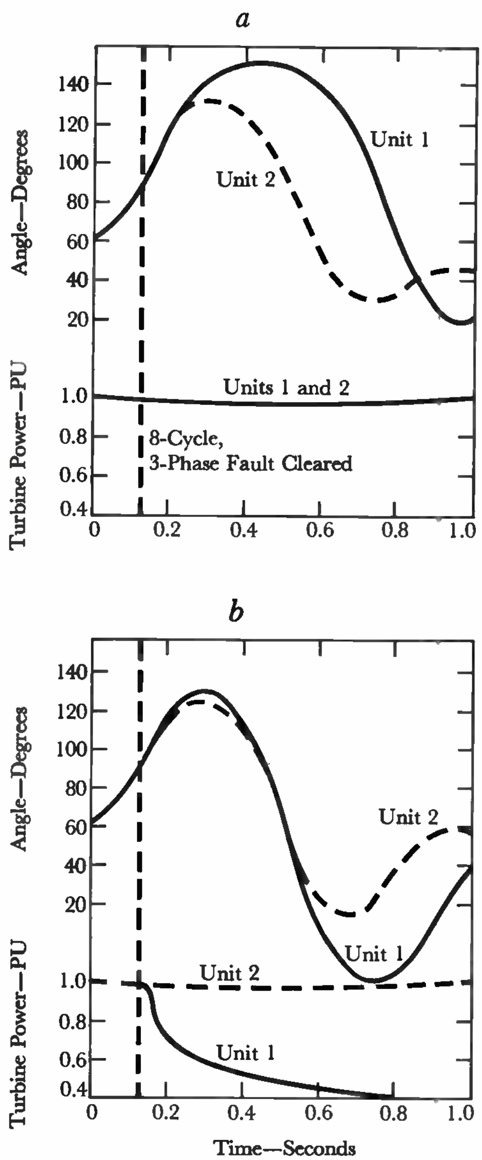

6—Effect of fast turbine valve closing upon generator angle swing: (*a*) no fast valving on either unit, and (*b*) fast valving on unit 1.

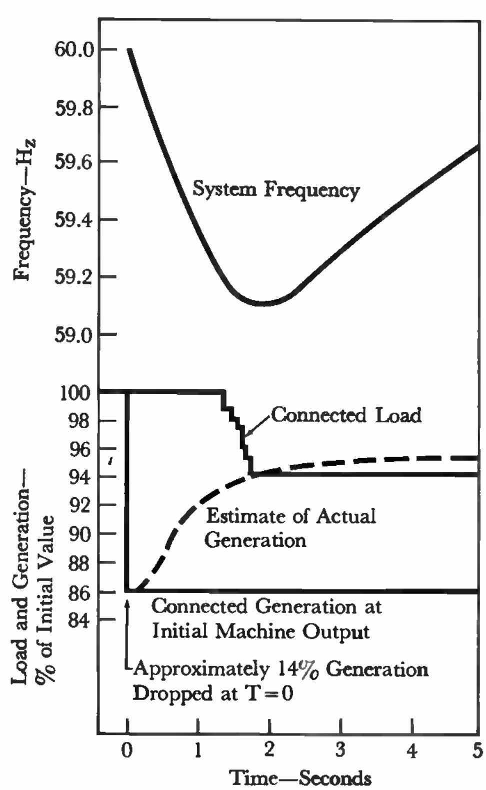

7—System response to loss of generation and subsequent load shedding. Governor response made up for part of generation loss.

shedding are provided by the program at each bus. For each bus, the criterion can be undervoltage or underfrequency and must be specified. For each load-shedding step, the threshold at which shedding occurs, a time delay before load is dropped after the threshold is reached, and a percentage of load to drop must also be specified. If frequency (or voltage) recovers before the delay time expires, load is not dropped, and the entire time delay must expire again if the frequency (or voltage) again drops below the threshold.

Some utilities have scheduled as much as 40 percent of their total load for load shedding. Such a scheme can be a powerful aid in preventing system collapse upon the loss of a significant amount of system generation. A typical system response following the loss of approximately 14 percent of generation is illustrated in Fig. 7. Although the initial generation deficiency was approximately 14 percent, only 6 percent of the load was shed. Load variation with voltage and frequency was simulated, but since voltages recovered to nearly rated value, voltage reduction did not account for any significant load reduction. Load variation with frequency was also very small. The major action to balance load and generation was increased generation through speed-governor response.

Input and Output Features

On large digital computer programs, organization of information is essential so that the magnitude of input data is kept reasonable and the output can be interpreted. This program will accept system load flow information from either input cards or magnetic tape, and it provides for two restart options that permit additional stability problems to be run from a load flow with a minimum of additional input data.

Input data is sorted and examined for errors, and a summary of it is printed out in clear tabular form for easy review. If errors are found, the appropriate diagnostics are printed out, and the computer run is terminated after initialization is completed. As the calculation progresses, solutions are stored on magnetic tape.

When a case is completed, the solutions are sorted so that all of the information for a given generator, bus, or transmission line can be tabulated concisely for the entire real time of the simulation.

A composite example of several printed page formats of output is shown in Fig. 8. All output items are stored on magnetic tape, and this feature allows automatic plotting by a cathode ray data plotter on either paper or microfilm. Curves of the rotor angles of up to 54 machines can be plotted on the same page or microfilm frame. Also available are larger plots of single-machine variables on a single page or frame of microfilm (Fig. 3 is an example of this type of output).

Conclusions

Recent advances in power system analysis techniques, typified by the new Westinghouse dynamic stability program, are made necessary by increases in system size, interconnection, and emphasis on reliability. The use of faster acting generator excitation and turbine governor systems are additional factors that contribute to this need.

Certain specific situations have also influenced the development of improved analytical methods. One of the most significant is the rapid growth of interconnection of operating companies in the western United States using both ac and dc EHV transmission systems. The interconnection planning studies for this region have given impetus to much of the program development over the past several years. The Northeast power failure of 1965 also stimulated development of techniques, particularly the ability to simulate automatic line tripping and reclosing during power swings or out-of-step conditions.

The new dynamic stability program reflects these needs by providing a more powerful analytical tool for tackling large system stability problems.


```
                                   OVER-ALL SYSTEM CONDITIONS

     TIME       NO. OF     TURBINE    ELECTRICAL   DAMPING   ACCELERATING  INF BUS      LOAD    GEN MINUS
              ITERATIONS  POWER SUM  GENERATION   POWER SUM     POWER     GENERATION   POWER      LOAD
     .000         1        1000.00     999.72       0.00          .28      -993.01      0.00      6.71
  BUS      3 FAULTED AT T =      .0000

     .000         6        1000.00      30.66       0.00       969.34        0.00       0.00     30.66
     .010         4        1000.00      27.50       1.24       971.26        0.00       0.00     27.50
  BUS      3 FAULT REMOVED AT T =    .0100

     .010        38        1000.00    1001.50       1.24        -2.74     -993.10       0.00      8.41
     .020        50        1000.00    1010.72       1.12       -11.84    -1006.06       0.00      4.66


                                      MACHINE VARIABLES

                           1     INDPT    1 0 UNIT
       GENERATOR    INTERNAL                 TERMINAL     TURBINE  ELECT     ACCEL   DAMP
     PER CENT ANGLE    VOLTAGE      CURRENT      VOLTAGE     POWER    POWER     POWER   POWER
  TIME FREQ DEV  DEG    MAG    ANG    MAG     ANG   MAG    ANG    MW       MW        MW      MW        VF       AUX
   .00  0.00     67 1.16     33    9.97      3  1.05     20  1000.0    999.7        .3    0.0     2.73     0.00
   .00  0.00     67 1.16     33   26.10    -56   .46     32  1000.0     30.7     969.3    0.0     2.73     0.00
   .01   .11     67 1.10     35   24.72    -53   .44     34  1000.0     27.5     972.5    1.2     2.77     0.00


                                          LINE FLOW

 FLOW FROM    2( TRANS    1 0 ) TO    1( INDPT    1 0 )
 TIME     P.U.VOLTAGE AT BUS    2   P.U. CURRENT       POWER FLOW           PER UNIT APPARENT   IMPEDANCE
 ____     ________________________  _____________  _________________________  ______________________________
  SEC.     REAL   IMAG   MAGN  DEGR.  MAGN    DEGR.  P MW     Q MVAR   S MVA   RESIST.   REACT.   IMPED.   ANGLE
   .000   .987   .224  1.012   12.8   9.97 -176.30 -997.02 -158.94 1009.61  -.1002   -.0160   .1015  -170.93
   .000   .056   .033   .065   30.4  26.10  123.82  -10.22 -170.28  170.59  -.0002   -.0025   .0025   -93.42
   .010   .052   .033   .062   32.6  24.72  126.03   -9.17 -152.76  153.04  -.0002   -.0025   .0025   -93.42
```

8—Sample output tabulations for system simulations made with the computer program.

Single-Zone Ground Distance Relaying

Leo Husak
G. D. Rockefeller

The SDGU Static Relay brings the flexibility of single-zone packaging to ground distance relaying.

Distance relaying is a desirable form of transmission-line protection because of its *reach stability*—the ability to protect to a constant distance regardless of what is happening on the system beyond the protected section. When a fault occurs on the system, each relay examines voltage and current conditions at its location to determine whether or not the fault is on the line section that it is protecting.

Distance relaying has been effectively applied for phase-to-phase fault protection, but it has not been particularly useful for ground faults when applied with conventional forms of nonreactance relays because of the unpredictability of ground fault resistance. Yet the need for effective ground distance relaying is evidenced by the fact that approximately 70 percent of all transmission line faults are single line to ground. Another impetus is the need for faster operating times for protecting EHV transmission lines from ground faults.

In looking for an effective ground distance relay, a primary objective was to achieve zone packaging similar to the K-Dar phase distance relaying system that has enjoyed wide acceptance.[1] This objective resulted in a new concept for ground distance relaying that utilizes the principles of symmetrical components. Introduced in 1965, the design approach has been proven both by staged fault tests and by in-service experience. The relay, called the SDGU or SDG, is zone packaged for complete stepped-distance protection. Thus, the flexibility enjoyed by single-zone phase-distance relaying is now available for ground fault protection.

Theory of SDGU System

The method of symmetrical components greatly simplifies the process of calculating short-circuit current and voltages. Basically, this technique consists of reduc-

L. Husak is a design engineer and G. D. Rockefeller is an Advisory Engineer at the Relay-Instrument Division, Westinghouse Electric Corporation, Newark, New Jersey.

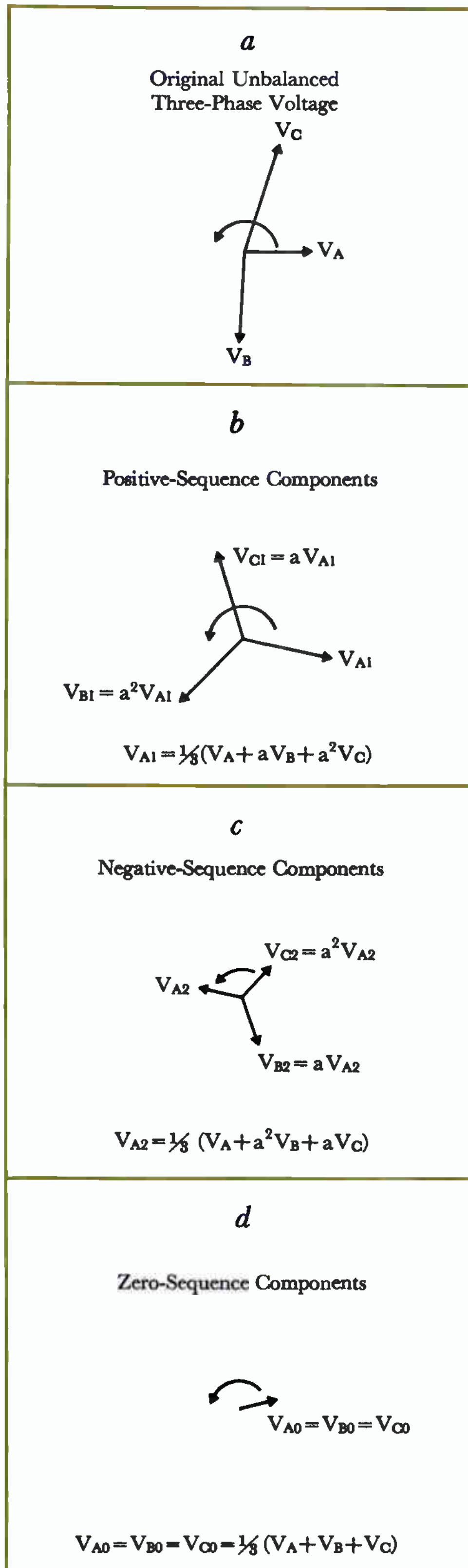

Symmetrical Components

The fundamental principle of symmetrical components, as applied to three-phase circuits, is that three unsymmetrical and unbalanced phasors of voltage or current (Fig. a) can be resolved into three sets of balanced phasors: ***positive-sequence*** components (Fig. b) consist of three phasors equal in magnitude, 120 degrees apart, and rotating in a direction so that they reach their positive maximum values in sequence *ABC*; ***negative-sequence*** components (Fig. c) are three phasors equal in magnitude, 120 degrees apart, but rotating in sequence *ACB*; and ***zero-sequence*** components (Fig. d) consist of three phasors equal in magnitude and ***in phase***. Thus, each set is a "symmetrical component" of the original unbalanced set of phasors, so that each original unbalanced phase phasor can be reconstructed from symmetrical component phasors.

The three unbalanced phase phasors of Fig. a are resolved into the symmetrical component phasors by use of the equations:

$$V_{A1} = 1/3\,(V_A + aV_B + a^2V_C)$$
$$V_{A2} = 1/3\,(V_A + a^2V_B + aV_C)$$
$$V_0 = 1/3\,(V_A + V_B + V_C),$$

where V_1 is the positive-sequence component, V_2 is the negative-sequence component, and V_0 is the zero-sequence component. The phasor operator (a) is of unit length and oriented 120 degrees in a positive direction from the reference axis ($a = -0.5 + j0.866$).

Conversely, the original unbalanced phase phasors can be expressed as functions of the symmetrical component phasors:

$$V_A = V_{A1} + V_{A2} + V_{A0}$$
$$V_B = V_{B1} + V_{B2} + V_{B0}$$
$$V_C = V_{C1} + V_{C2} + V_{C0}.$$

Three unbalanced line currents are resolved into three sets of symmetrical components in the same fashion.

When applying symmetrical components to circuit analysis, an impedance network is set up for each symmetrical component, and the quantities Z_1, Z_2, and Z_0 are the impedances of the system to the flow of positive-, negative-, and zero-sequence currents, respectively. These characteristic impedances vary with the type of equipment and must be derived for the particular circuit under consideration.[2,3]

Unbalanced impedances that occur during system faults or unbalanced loads also can be resolved into symmetrical components. These impedances are phasor operators rather than the rotating phasors of three-phase voltage and current.

1

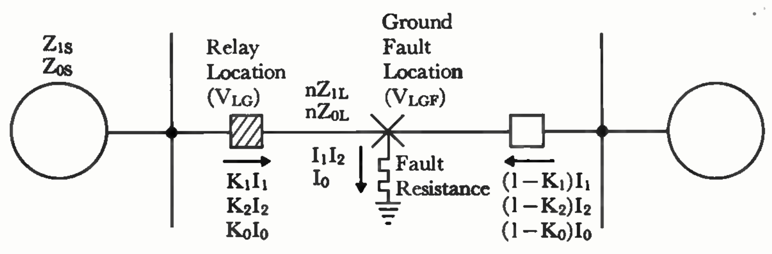

2

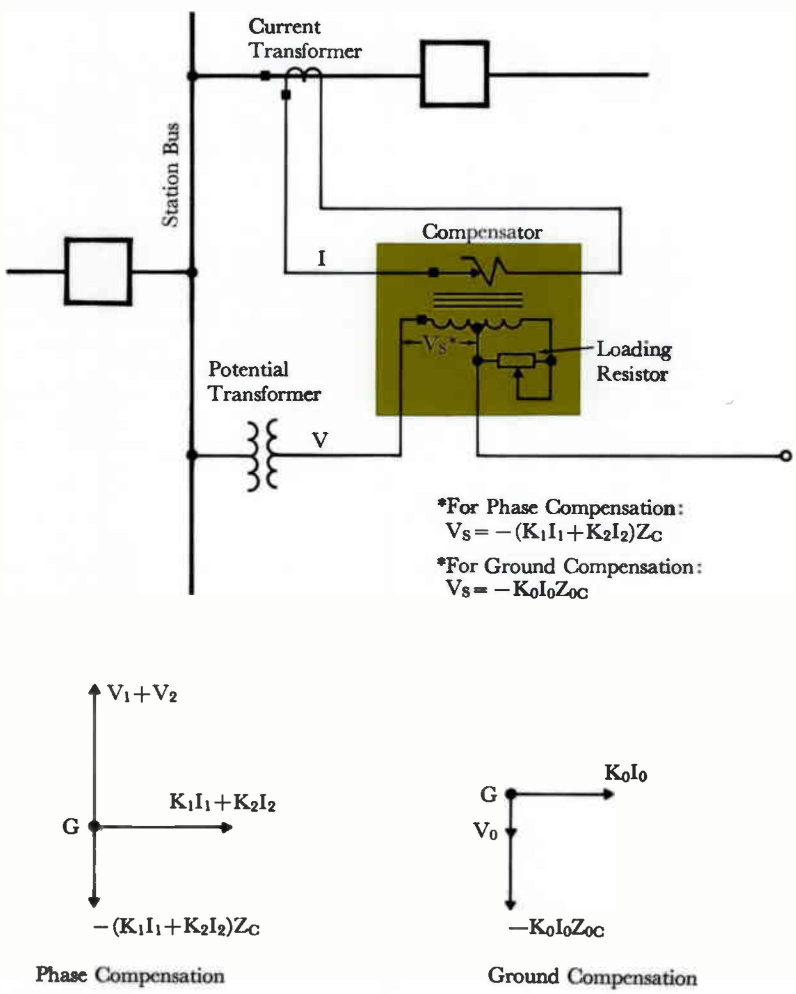

ing an unbalanced three-phase system of vectors into three balanced sets of vectors called positive-, negative-, and zero-sequence phase components. (See *Symmetrical Components*, preceding page.) Since sequence voltages and currents can be conveniently segregated and measured by appropriate instrumentation, these sequence components can provide information for relaying. The SDGU ground distance relaying system uses a very basic sequence-component relationship that exists at the fault point of a grounded phase.

Neglecting fault resistance, the line-to-ground voltage at a fault is zero. Thus, the symmetrical component voltages that make up the faulted-phase voltage (V_{LGF}) at the fault must equal zero:*

$$V_{LGF} = V_{1F} + V_{2F} + V_{0F} = 0.$$

Therefore,

$$V_{1F} + V_{2F} = -V_{0F}, \text{ and}$$
$$|V_{1F} + V_{2F}| = |V_{0F}|.$$

In other words, the *magnitude* of the sum of the positive- and negative-sequence voltages must equal the *magnitude* of the zero-sequence voltage *at the fault*. As will be shown, this basic relationship is the key to the SDGU ground distance system.

*Throughout this article, the subscripts 1, 2, and 0 refer to positive-, negative-, and zero-sequence components respectively. The subscript F denotes quantities *at the fault point*.

1—Positive-, negative-, and zero-sequence currents and impedances for a line-to-ground fault are illustrated.

2—Compensators are essentially air-gap transformers that subtract a replica of the fault-current line impedance drop from phase voltage at the relay to reproduce the phase voltage existing at the preset balance point. Positive- and negative-sequence components are used for phase compensation, and zero-sequence components are used for ground compensation.

3—Phasor diagrams illustrate the development of *(a)* restraint voltages and *(b)* operating voltage for a phase-A-to-ground fault within the operating zone.

4—The voltages developed *at the relay* for several phase-A-to-ground fault locations illustrate the relationships between restraint voltage (V_{XN}) and operating voltage (V_{WO}).

3a

b

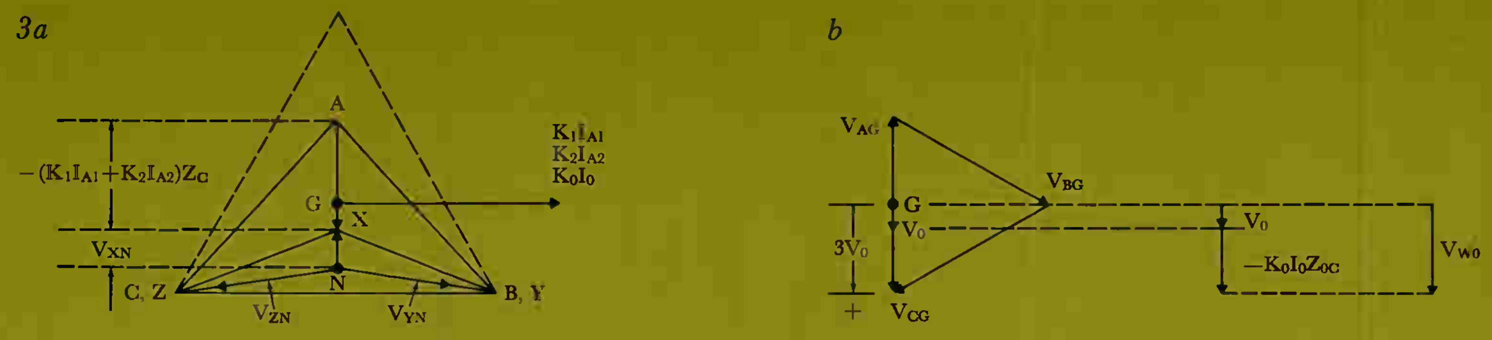

Restraint voltages, V_{XN}, V_{YN}, V_{ZN}
(N is at centroid of restraint triangle.)

Operate Voltage V_{W0}

4

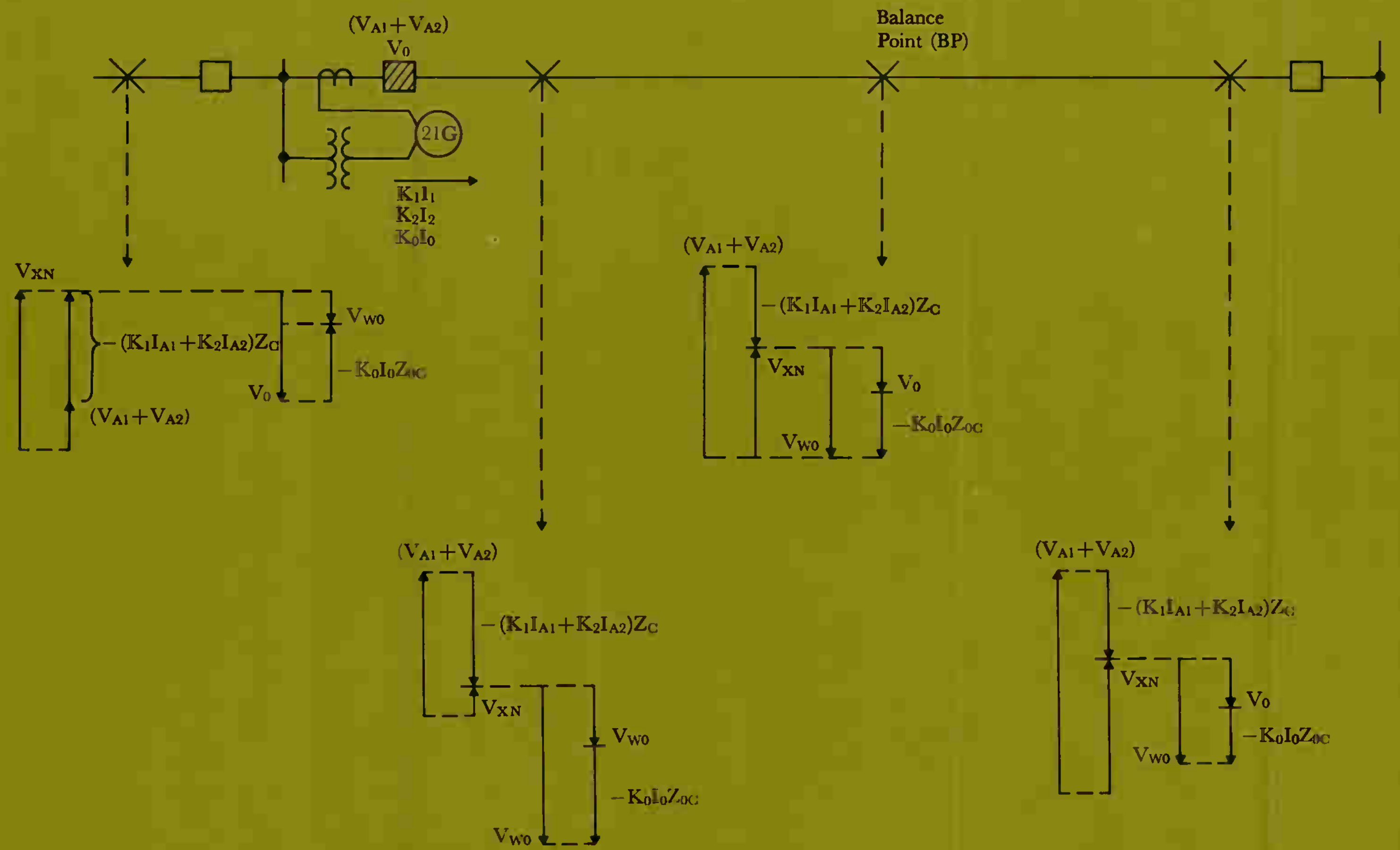

The faulted-phase voltage *at the relay* will be greater than zero because of the line impedance drop between the relay location and the fault. Expressed in terms of symmetrical component currents for the faulted phase, the line-to-ground voltage at the relay is:

$$V_{LG} = K_1 I_1 n Z_{1L} + K_2 I_2 n Z_{1L} + K_0 I_0 n Z_{0L},$$

where K_1, K_2, and K_0 are current distribution factors for the positive-, negative-, and zero-sequence networks (Fig. 1), I_1, I_2, and I_0 are the sequence currents *in the fault*, and nZ_{1L} and nZ_{0L} are the positive- and zero-sequence line impedances from the relay to the fault (for transmission lines, positive- and negative-sequence impedances are equal).

Line-drop compensators (to be described later) develop replicas of the fault-current line impedance drops *at the relay location;* the phase replica voltage drops are subtracted from the phase voltages at the relay, thereby reproducing the phase voltages existing at a preset fault point (balance point) on the transmission line. Using these reproduced fault-point voltages, the relay compares the magnitude of the positive- plus negative-sequence voltages with the magnitude of the compensated zero-sequence voltage to determine whether the fault is on the relay side of the balance point (producing an *operate* signal) or on the far side of the balance point (producing no output).

SDG/SDGU Application Guide

Rack Type (Note 1)	Flexitest Case Type	Application	I_0 Fault Detector	Frequency Verifier	Two-Phase-to-Ground Desensitizer	Output
..	SDG (Note 2)	Zone 1	√	√	√	Thyristor
SDGU-1	..	Zone 1	√	√	√	Transistor
SDGU-2	..	Zone 1 (Note 3)		√	√	Transistor
SDGU-3 (Note 4)	SDG-3 (Note 4)	Zone 2 or 3 timed trip	√			Transistor
SDGU-4	..	Blocking start				Transistor
SDGU-5	..	Pilot trip		√		Transistor

Notes:
1. Standard 19-inch rack mounting.
2. Self contained except for SPP and TP-1 surge protection. Use with electromechanical relays.
3. Use where SIU relay provides current supervision.
4. Use with TD-50 timer (one timer per zone).

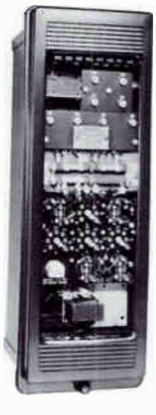
SDG


SDGU

Relay Restraint Voltage

For a fault at the balance point, the *restraint* voltage for the relay represents the sum of the positive- and negative-sequence voltages ($V_{1F}+V_{2F}$) for the faulted phase. The restraint voltage is obtained by the use of compensators with impedances (Z_C) set to match the positive-sequence line impedance to the desired balance point.

Compensators are essentially air-gap transformers with current-energized primary windings (Fig. 2) that induce the replica voltages in the secondary windings. For purposes of illustration, this replica voltage is shown lagging the current by 90 degrees. In practice, the loading resistance is adjusted so that the replica voltage approximately matches the line impedance drop angle. Bus voltage is applied to the input of the secondary windings, and a voltage proportional to the product of line impedance to the balance point and system current flowing in the primary winding is subtracted phasorally from bus voltage, providing a difference voltage at the secondary output terminal of the compensator.

Compensated voltages on the three phases energize an ungrounded-neutral auxiliary transformer. Since currents flowing into a Y-connected transformer cannot have a zero-sequence component unless the neutral is returned or grounded, only positive- and negative-sequence components appear at the output of the auxiliary transformer. For grounded phases, the restraint voltage will be:

$$V_{FN} = (V_1 + V_2) - Z_C(K_1 I_1 + K_2 I_2),$$

where V_{FN} is one of the three restraint voltages V_{XN}, V_{YN}, or V_{ZN} to be described. Thus, the restraint voltages for grounded phases duplicate the positive- plus negative-sequence voltage components *at the fault* ($V_{1F}+V_{2F}$) when the fault is Z_C ohms from the relay (i.e., at the balance point). The development of this restraint voltage is illustrated with the phasor diagram in Fig. 3a.

Restraint voltages are similarly produced for unfaulted phases. Only the *lowest* restraint voltage (V_{XN} in Fig. 3a) is used for voltage magnitude comparison by the relay.

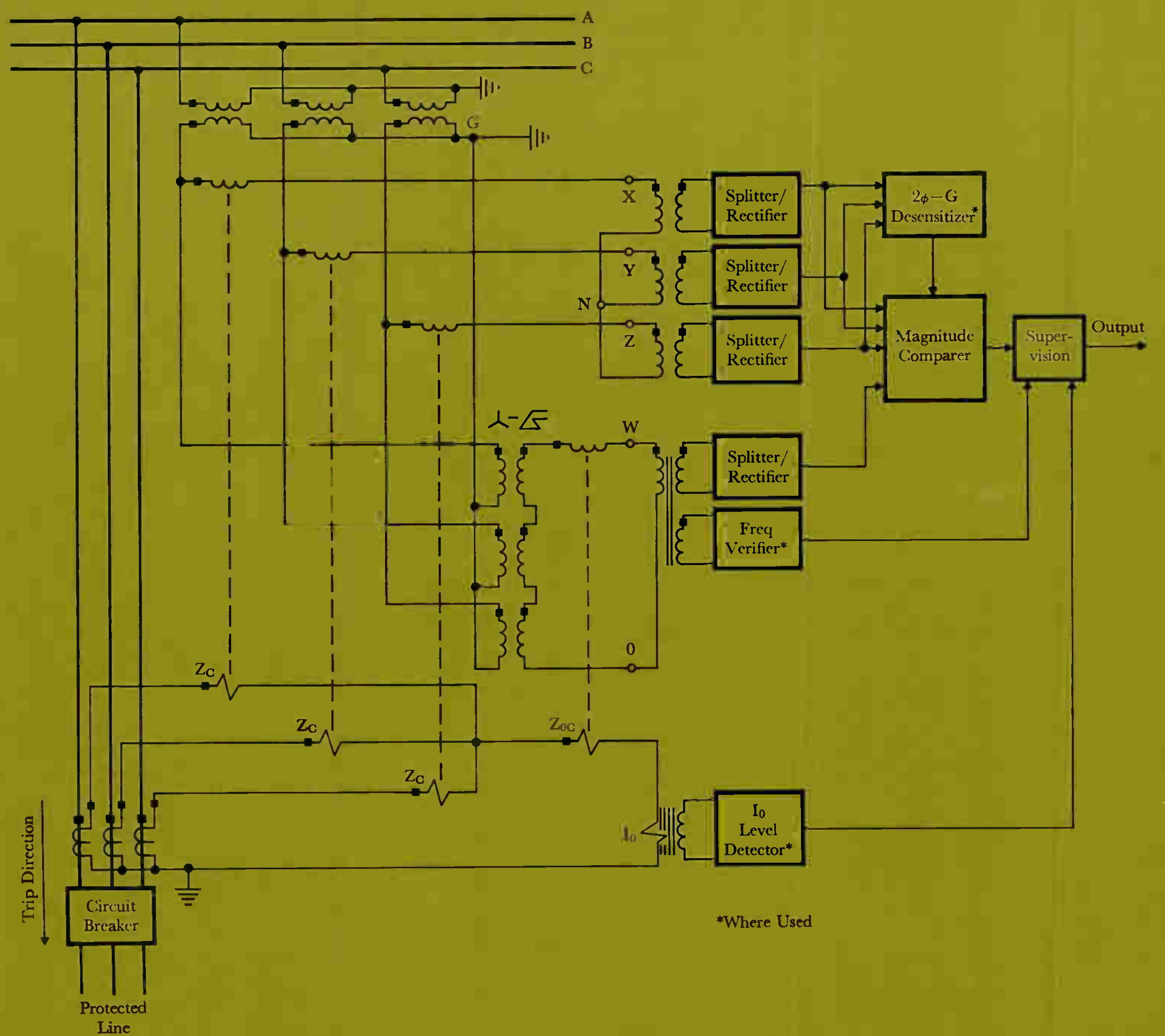

5—Block diagram of SDGU (or SDG) ground distance relaying system. Positive- plus negative-sequence restraint voltages for each of the three phases and the zero-sequence operating voltage are developed by ac circuitry (left side of diagram); dc circuitry (right) compares the voltages to determine if output is called for. If operating voltage exceeds any phase restraint voltage, the relay operates.

Operating Voltage

Relay *operating voltage* (V_{W0}) represents the zero-sequence voltage at the fault for a balance-point fault. The operating voltage is developed by compensating the zero-sequence component of bus voltage, which is developed from the three secondary windings of an autotransformer connected in broken delta. Since a broken delta produces a zero-sequence component for each phase, or $3V_0$, the primary-to-secondary turns ratio is three to one to provide the desired zero-sequence voltage magnitude. Another compensator phasorally subtracts the zero-impedance line drop from the zero-sequence voltage component at the relay to reproduce the zero-sequence voltage component at the fault, or:

$$V_{W0} = V_0 - K_0 I_0 Z_{0C},$$

where compensator impedance (Z_{0C}) represents the zero-sequence line impedance to the desired balance point. For a ground on the protected line, impedance-voltage subtraction essentially results in an arithmetic addition because of the phasor relationships between the voltages and currents involved, illustrated in Fig. 3b.

The development of restraint and operating voltages for phase-A-to-ground faults are shown in Fig. 4. The voltages are shown for faults at key points on the system, but note that the figure depicts the voltages as developed *at the relay* rather than at the fault location.

Restraint-Operating Voltage Comparison

A block diagram of the dc circuitry used for comparing restraint and operating voltages is shown in Fig. 5. The positive-plus negative-sequence restraint voltages developed for each of the three phases and the zero-sequence operating voltage are fed to phase-splitter/rectifier circuits that provide dc outputs; these outputs are compared in a magnitude-comparison circuit. If the operating voltage $|V_{W0}|$ exceeds any one of the phase restraint voltages, $|V_{XN}|$, $|V_{YN}|$, or $|V_{ZN}|$, the relay operates.

A two-phase ground-fault desensitizer prevents the relay from overreaching on double-line-to-ground faults in the presence of interphase arc resistance. This resistance distorts the current-impedance phasor relationships in the compensators for a DLG fault. The desensitizer circuit reduces the reach of the relay about 15 percent during DLG faults.

The desensitizer senses a DLG fault by noting that two of the three restraint voltages are smaller than the third. For single-line-to-ground faults near the balance point, one of the restraint voltages is smaller than the other two and the desensitizer circuit is blocked.

For high-speed trip applications, a *frequency-verifier* circuit prevents tripping

R-X Characteristic for Distance Relay

The simplest form of R-X characteristic can be illustrated by the classic single-phase balanced-beam impedance element, many of which are still in service. Relay restraint is provided by phase voltage, and relay operating torque is provided by phase current. The relationship between voltage and current, as seen by the relay, is an impedance ($Z = V/I$). At the relay balance impedance (Z_{BP}), the restraint provided by voltage equals the operating torque provided by current. Since the balance is mechanical, phase angle between voltage and current has no effect on relay performance, and the tripping characteristic, plotted on an R-X diagram, is a circle of radius Z_{BP}. Thus, the element is nondirectional. When the impedance seen by the relay is less than its balance impedance (inside the Z_{BP} circle), the relay trips; when greater than Z_{BP}, the relay does not trip.

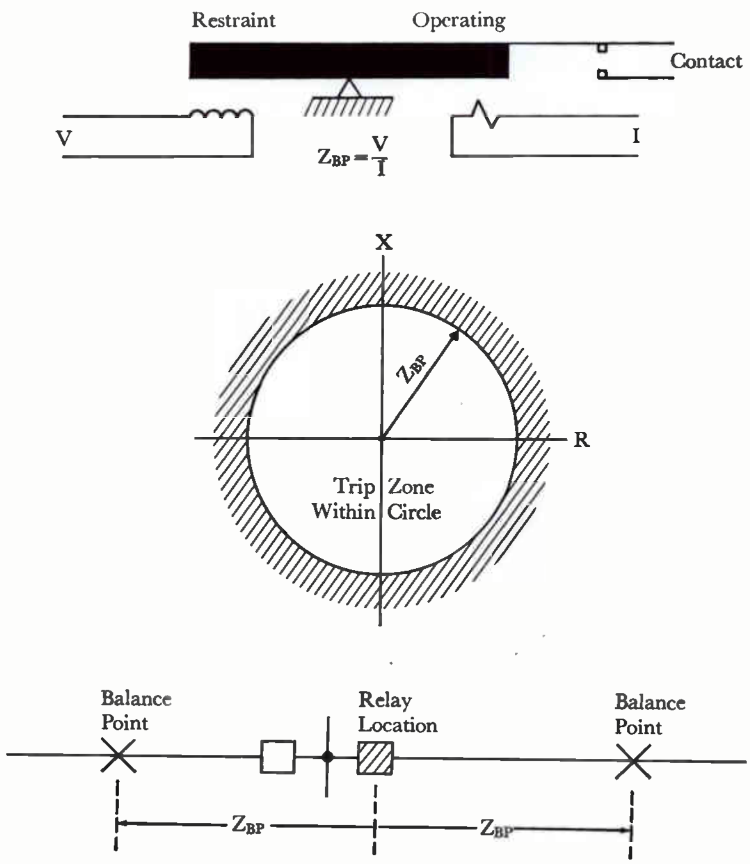

6—*(Right)* **SDGU relay R-X diagrams for single-line-to-ground faults are illustrated for** ***(a)*** **long-line,** ***(b)*** **medium-length-line, and** ***(c)*** **short-line applications.**

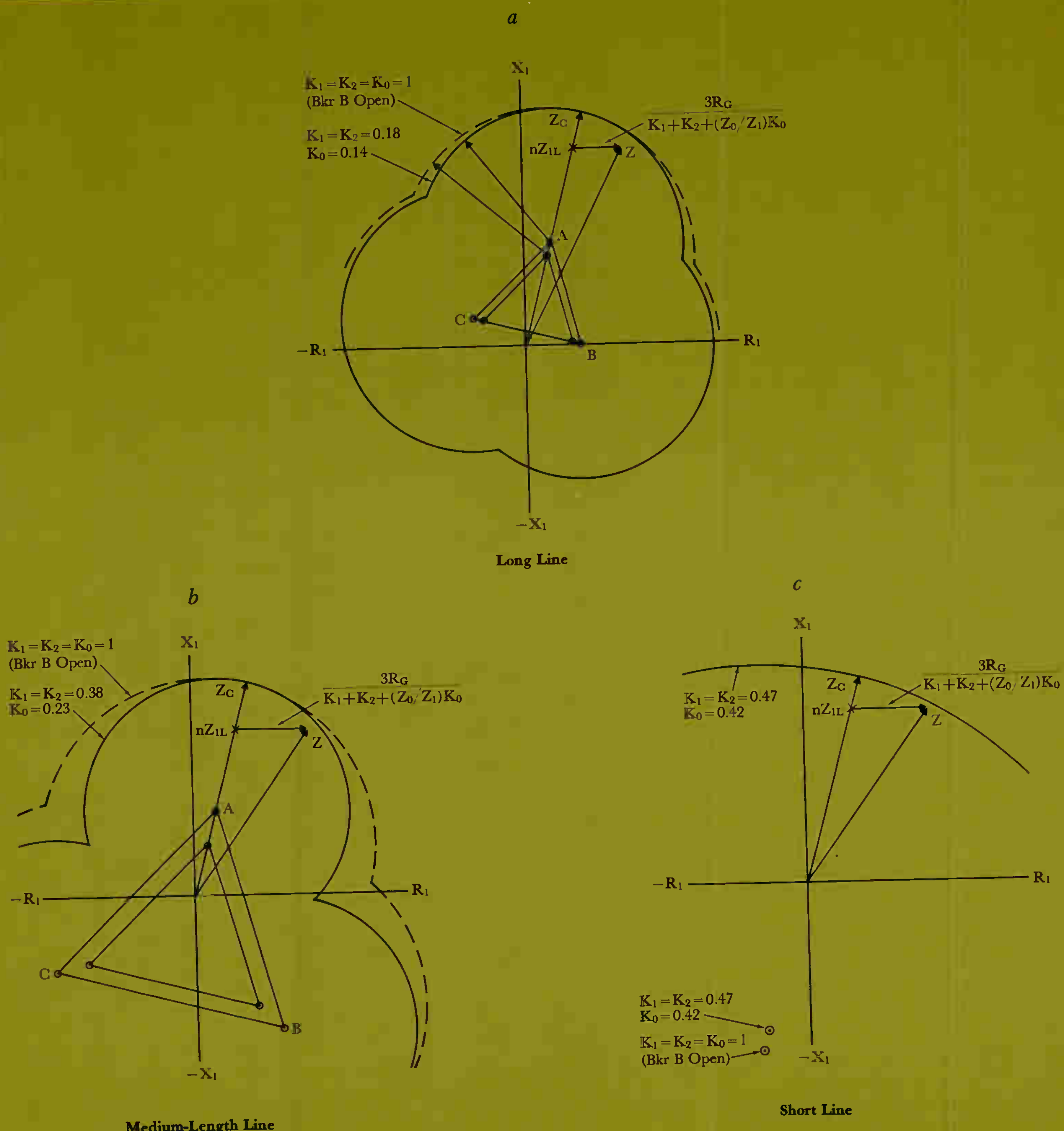
a
X1
K1 = K2 = K0 = 1
(Bkr B Open)
K1 = K2 = 0.18
K0 = 0.14
ZC
3RG
K1+K2+(Z0/Z1)K0
nZ1L
Z
A
C
B
−R1
R1
−X1
Long Line
b
K1 = K2 = K0 = 1
(Bkr B Open)
X1
K1 = K2 = 0.38
K0 = 0.23
ZC
3RG
K1+K2+(Z0/Z1)K0
nZ1L
Z
A
−R1
R1
C
B
−X1
Medium-Length Line
c
X1
3RG
K1+K2+(Z0/Z1)K0
ZC
K1 = K2 = 0.47
K0 = 0.42
nZ1L
Z
−R1
R1
K1 = K2 = 0.47
K0 = 0.42
K1 = K2 = K0 = 1
(Bkr B Open)
−X1
Short Line

on voltage transients that occur during line-energizing or fault-clearing operations. The circuit provides an output that permits tripping if the operating voltage period (between zero crossings) exceeds four to five milliseconds. Thus, any voltage of more than about double frequency cannot produce tripping. The frequency-verifier circuit works simultaneously with the magnitude-comparison circuit so that no unnecessary delay is introduced. Of course, operation can never be faster than four to five milliseconds when the frequency-verifier circuit is used.

A zero-sequence *fault current detector* can be used to prevent relay tripping on a partial loss of voltage due to potential-circuit trouble. This circuit has a fixed 0.4 ampere residual-current pickup. This pickup value is the minimum safe value to avoid operation on normal load unbalances.

When AND inputs are present from the magnitude-comparison circuit and all optional circuits in use, the decision-making circuit provides a 20-volt output signal. This signal can be used to gate an external thyristor circuit that will trip the breaker, to work into other solid-state logic, or to key a carrier transmitter. Optional circuit combinations and their application are given in the table, p. 120.

Distance Characteristics

The SDGU ground distance characteristic for single line-to-ground faults is shown on an R-X diagram in Fig. 6. The apparent impedance (Z) that the relay sees must fall within this characteristic for the relay to operate. The apparent impedance is:

$$Z = nZ_{1L} + \frac{3R_G}{K_1 + K_2 + (Z_0/Z_1)K_0},$$

where nZ_{1L} is the positive-sequence line impedance from the relay to the fault and the second term is the fault resistance component.

The relay R-X characteristic is a composite of three impedance circles, one for each phase, with offsets *A*, *B*, and *C*. The impedance circle with center *A* is produced from the comparison of faulted-phase restraint and operating voltage and is similar to a conventional modified impedance characteristic. The *B* and *C* circles result from the unfaulted-phase restraint comparisons with operating voltage.

The offset and radius of each impedance circle are derived mathematically and are a function of both source and line impedances. Thus, as the ratio between source impedance and line impedance changes, the offset and radius of the impedance circle also changes. R-X characteristics are shown for a long line where source impedance is low compared with line impedance, a medium-length line, and a short line where the source impedance is high compared with the line impedance.

Regardless of the ratio of source impedance to line impedance, the relay reach is determined by compensator impedance (Z_C) for a fault at the compensator angle. The expansion of R-X circle diameter with increasing source impedance is beneficial because it provides increased fault resistance accommodation for the shorter line applications where the fault resistance can be large compared with line impedance. Thus, a greater fault resistance component is required to yield a Z-phasor that is outside the operate zone.

Although the relay R-X characteristic diagram includes the origin and suggests that the relay is not directional, this is not actually the case for the SDGU relay. The mathematics[4] assumes that the fault is in the trip direction. For a fault behind the relay, the characteristics shown in Fig. 6 do not apply. Thus, the second and third quadrants of the R-X diagram are essentially theoretical because relay operation in these quadrants could only occur for a "negative resistance." The fourth quadrant (with negative reactance) is only pertinent for series capacitor applications. Thus, only the first quadrant of the relay R-X characteristic is generally applicable.

Application of SDGU Relays

The SDGU ground distance relay is applied as an impedance-type relay with a modified impedance characteristic. Special circuitry prevents incorrect operation due to over-frequency, line oscillations, loss of voltage, or double-phase-to-ground faults. With these refinements, high speed operation of 7 to 11 milliseconds is obtained without sacrificing system security.

The offset impedance characteristic of the SDGU relay allows the Zone 1 relay reach to be set to 85 percent of the protected line. Being inherently directional, the SDGU relay does not require any extra components for directional supervision.

Zone packaging allows great flexibility in designing a relay system for multiple zone primary and backup protection.[4,5] With SDGU relays, a single zone or any number of zones can be applied.

On short lines, the SDGU relay provides better instantaneous coverage and faster end-zone clearing times than does a directional-overcurrent relay. The Zone 1 distance reach is not affected by external system variations as is an overcurrent relay.

For step-distance protection, the Zone 2 relay with its controlled reach can be set with timers to coordinate with the instantaneous zone of adjacent lines to achieve fast end-zone clearing times. These relays are used in various pilot systems.

With a single-zone multiphase unit, the relay engineer can solve his relaying problem with a minimum of complexity. For example, existing overcurrent relaying can be upgraded by simply adding an SDG Zone 1 distance relay. This kind of building-block flexibility has already proved advantageous in K-Dar phase distance relaying and is now available for ground fault protection, either pilot or nonpilot.

Westinghouse ENGINEER **July 1969**

REFERENCES:

[1] H. W. Lensner, "K-Dar Compensator Relaying," *Westinghouse ENGINEER*, July 1959, pp. 114-8.

[2] *Applied Protective Relaying*, published by Relay Department, Westinghouse Electric Corporation, Newark, New Jersey.

[3] *Electrical Transmission and Distribution Reference Book*, Westinghouse Electric Corporation, East Pittsburgh, Pennsylvania.

[4] G. D. Rockefeller, "Zone-Packaged Ground Distance Relay. I—Principles of Operation," IEEE Paper 31 TP 66-122.

[5] H. J. Calhoun and L. Husak, "Zone-Packaged Ground Distance Relay. II—Design and Performance," IEEE Paper 31 TP 66-123.

Side-Look Radar Mapping Now Used for Geological Reconnaissance

Airborne side-look radar mapping, developed as a military reconnaissance tool, is now being used for geological reconnaissance to aid in oil and mineral exploration. The system's radar pulses are beamed downward and to the side of the aircraft, and energy reflected from the ground back to the aircraft is converted to light and recorded on photographic film as photo-like imagery of the ground.

The radar system was designed and built under Department of Defense sponsorship and U.S. Army management by the Westinghouse Defense and Space Center, which then leased it from the Army and installed it in its own DC-6B aircraft. It is part of the company's earth resources radar geological reconnaissance service.

The system amplifies the reflected signals, which vary in intensity according to the ground conditions they encountered, and displays them on a cathode-ray tube. A strip of photographic film passes across the face of the tube and records the image of the ground line by line. Film speed and airplane ground speed are synchronized. The antenna subsystem is mounted below the airplane and gyro-stabilized so that movements of the airplane do not affect accuracy of the imagery. (For more information about side-look radar, see "All-Weather Mapping by Radar," A. A. Nims, *Westinghouse ENGINEER*, May 1968, pp. 76-81.)

The system is an efficient diagnostic tool that helps earth scientists understand the earth's crust. Before a geophysicist goes to the expense and trouble of detailed exploration, such as seismic mapping, he tries to find regions that are likely to be good areas for close study. He usually does so by examining surface features, and that is where the airborne radar system comes in. It quickly provides imagery that can be interpreted in a number of ways to provide a great deal of reliable information about geological surface features over large areas. Those surface features help indicate the nature of the subsurface structures, so they help the geoscientist draw conclusions about the potential presence of mineral or hydrocarbon deposits.

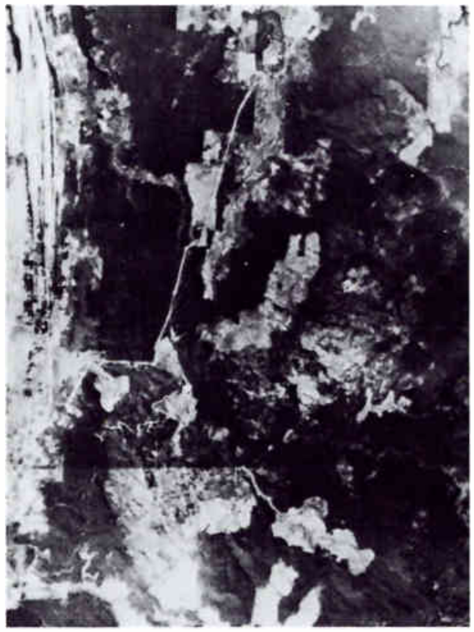

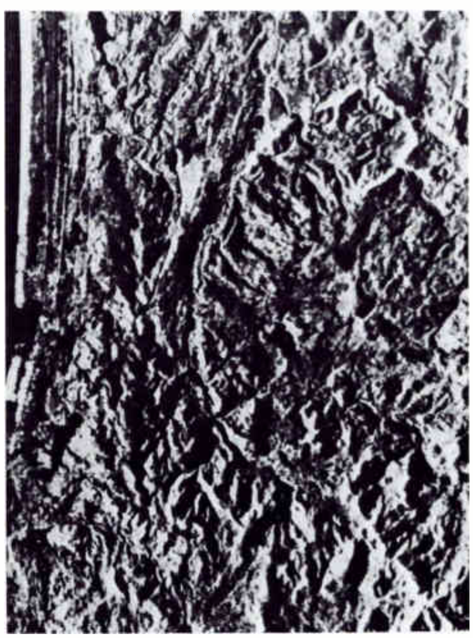

Composite aerial photograph *(top)* and side-look radar imagery *(bottom)* show the same area near Seaside, Oregon. The radar imagery reveals a large curved geological structure in the center of the picture that does not show in the aerial photo and was not known to exist. (The aerial photography was made in April 1956; the radar imagery in October 1965. North is at the top.)

Side-look radar imaging is especially useful for areas that have never been geologically mapped and where climatic conditions are adverse for aerial photography. It can also be useful for restudying areas already explored.

Moreover, terrain features not detectable in other ways are apparent in radar imagery, simply because the system uses a different part of the electromagnetic spectrum. For example, the degree of depolarization of a radar return signal, which is influenced by the nature of the object it struck, is detectable. The system has one transmitter and dual antennas and receivers so it can receive cross-polarized return signals and, at the same time, signals that have the original polarization. Cross-polarized signals appear on one half of a strip of imagery and like-polarized signals on the other to permit direct comparison of the two images. (See photo on outside back cover.)

Nuclear-Plant Training Center Has Simulator plus Actual Plant

A center to provide basic training and periodic retraining of operators for all nuclear power plants having pressurized-water reactors will be built by Westinghouse and Commonwealth Edison Company at Zion, Illinois. It is scheduled for operation in 1971 and will be the largest and most versatile facility of its kind in the world. It will be located near the Commonwealth Edison nuclear power station now under construction at Zion. Commonwealth Edison will supply the land and the 30,000-square-foot building for the training center, and Westinghouse will equip, staff, and operate it.

The key training aid will be an advanced electronic nuclear-plant simulator built around a Prodac 2000 process control computer. Other facilities will include a training reactor, a television studio for producing videotaped lectures, three classrooms, a library, a training materials unit, and administrative offices. The simulator will be programmed to duplicate the unique features of the particular nuclear power plant for which each group of operators is being trained; its versatility will permit the training of more than 200 people a year.

Moreover, the 2.2-million-kW Zion station will be made available to prospective operators for training by observation. The station will have two Westinghouse pressurized-water reactors in operation by 1973.

The center's basic and refresher training programs will be designed especially to prepare prospective operators for the rigorous written, oral, and practical examinations required for Atomic Energy Commission operator licenses. In addition, however, it will offer courses in nuclear reactor technology for nonoperating utility personnel. Special courses will also be provided for plant engineering staffs, instrumentation technicians, and health physics technicians.

Circuit Breaker Duty Program Facilitates Application Evaluations

Evaluation of circuit-breaker ratings for an electric power system is based on the magnitude of available fault current at the breaker locations, whether the evaluation is for the purpose of choosing ratings for a new installation or checking an existing installation for adequacy of breaker capacity. The maximum available fault current at a particular location is generally composed of an ac (or symmetrical) component and a dc component. Both components are considered by present methods of rating breakers, and both should be considered in applying breakers or in determining the duty on existing breakers.

The Westinghouse short-circuit digital computer program has provided an accurate and efficient method of calculating symmetrical fault current, and now that program has been supplemented by a circuit breaker duty program at the company's Power Systems Planning Department. The breaker duty program uses results of a digital short-circuit study to determine the dc component of fault current associated with the maximum value of symmetrical fault current at a particular breaker location, and then it computes the maximum value of total rms fault current available there.

The program considers breaker contact-parting times and actual system X/R ratios, so values indicative of both momentary and interrupting duties can be calculated. Printed output from the program can be used to evaluate the application of breakers rated on the new "symmetrical current" basis or on the older "total current" basis.

The ac component of fault current computed by the short-circuit program is a symmetrical current, determined primarily by internal reactances of the motors and generators in the system and by external system impedances. The internal reactances of machines may change appreciably during a fault, giving rise to a change in the ac component of fault current. This ac decrement can be considered in the short-circuit study by proper representation of the generators and motors.

The primary job of the breaker duty program is to calculate the dc component of total fault current. The dc component is an offset in the total fault current, brought about because inductance in the power system circuits opposes any instantaneous current change. Rigorous calculation of the total fault current as a function of time following a fault shows that the dc component decays at a rate determined by the sum of several exponential terms. However, rigorous calculation for faults on a general network is prohibitively complex, even with digital methods, so it is usually abandoned for less complicated approximate techniques that yield results of sufficient accuracy for most breaker applications. The circuit breaker duty program employs such an approximate method, involving the reduction of a system to an equivalent resistance (R) and reactance (X) as seen from the point of fault. The decay of the dc component is then determined by one exponential term whose time constant is proportional to the X/R ratio of the reduced network.

Fault current values computed in this manner have been found to be always somewhat less than values computed by rigorous methods. To compensate, the breaker duty program computes an estimated error and a corresponding correction factor that is applied to the fault current. Inclusion of the correction factor, which may vary between zero and eight percent, insures that the value of total fault current in the printed output contains at most an error on the conservative side.

Intrusion Detection System Keeps Ear to Ground

Small vibrations generated by footsteps create pressure waves in the surface of the earth, and engineers have now made use of the waves in an automatic property protection system that detects intruders crossing a designated area. Placed around the perimeter of a factory, unattended pumping or power station, or any other property, the Periguard Intrusion Detection System's sensitive transducers detect trespassers from any direction.

Fluid-filled sensor hoses are buried in the soil along the boundaries of the area to be protected. The hoses serve as hydraulic media for registering changes in ground pressure, and thus the presence of

A typical control and display console for monitoring several Periguard units portrays the system's layout, with lamps identifying the various units of the system. When an intruder is detected, the appropriate lamp identifies the area being crossed.

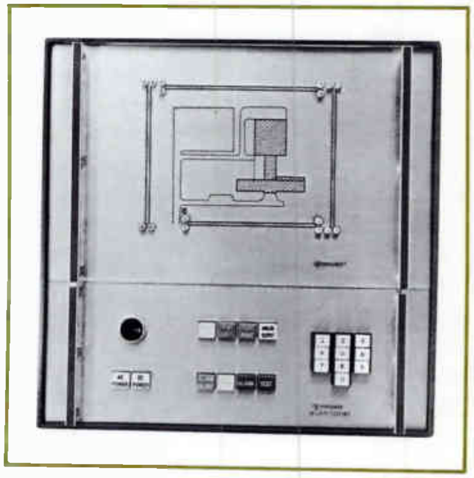

an intruder, while remaining hidden. They are buried in pairs along parallel paths several feet apart. A single Periguard unit can monitor several hundred feet of perimeter; longer perimeters are protected by a chain of units.

Pressure waves received by the hoses are transmitted through the fluid to underground detector units, containing transducers, at the ends of the hoses. Each transducer consists essentially of a diaphragm with a disc of piezoelectric material bonded to its center. When the diaphragm is bulged outward by pressure waves in the hose, the piezoelectric disc undergoes considerable radial stress and therefore generates relatively large electrical signals from small pressures. The signals are amplified and sent through underground cables to a control and display location.

The transducer's sensitivity to pressure changes becomes less as static pressure within the hose increases. That compensation feature is necessary for relatively constant intrusion sensitivity, because intrusion signals are more effectively coupled into and propagated along the hose as static pressure increases with soil compaction and with seasonal temperature changes. The compensation is provided by the diaphragm, which is rather flexible when not under pressure but becomes stiffer with deflection.

The gain of the integrated-circuit amplifier can be adjusted externally to fix the sensitivity of the system as required by the application. The output can activate various types of indicators, such as buzzers and lights on a console that indicates which hose unit is sending an alarm. The amplifier output can also be used to energize relays for such optional equipment as floodlights and television.

Since the hoses are buried in pairs, distant disturbances such as heavy traffic, sonic booms, and seismic waves affect each hose equally. Those signals immediately cancel at the detector unit because the transducers there have opposite polarity. (Transducer outputs are equal but opposite for the same pressure input.) However, an intruder approaching the perimeter is closer to one hose than to the other, so the signal strengths in the two hoses are correspondingly strong and weak. The detector sends an alarm to the control and display console only when signal strength is significantly different in the two hoses.

The Periguard Intrusion Detection System is manufactured by the Westinghouse Specialty Electronics Division. It is an outgrowth of long-time research programs in sonar and other acoustic devices conducted by the company's Research Laboratories.

Air Force Tactical Radar Is Mobile and Reliable

The U.S. Air Force's newest tactical radar is a long-range ground-based system built to meet stringent mobility and reliability requirements. The radar, designated AN/TPS-43, is part of the 407L tactical air control system. It was developed and is being built for the Electronics Systems Division of the Air Force Systems Command by the Surface Division of the Westinghouse Defense and Space Center.

For ease of transportation, the system is built in two units, each of which weighs 3500 pounds. The units can be transported in a variety of ways, including helicopter transfer. In mobility tests, technicians assembled a system and had it in operation in 36 minutes—well under the one-hour design requirement.

In a reliability test, a system was operated continuously for 1000 hours over a period of 7 weeks. One hour each day was alloted for preventive maintenance but, in several instances, the system was operated for a full 24 hours. High reliability is achieved through extensive use of solid-state components. Only 12 electronic tubes are used, with about 3000 integrated circuits and 1200 transistors.

The AN/TPS-43 is a three-dimension system; that is, it computes and displays the altitude of a target aircraft in addition to the usual bearing and range information. It is capable of detecting aircraft to a range of 120 nautical miles.

Digital techniques are used for signal processing, eliminating the frequency drift problems normally encountered in analog signal comparison circuits. A digital moving-target indicator operates in conjunction with a coded pulse anticlutter system to reject clutter and identify moving targets. The digital features make the radar system compatible with the most advanced automatic control centers. Since it also has analog outputs, it can be used with manual display and unautomated procedures.

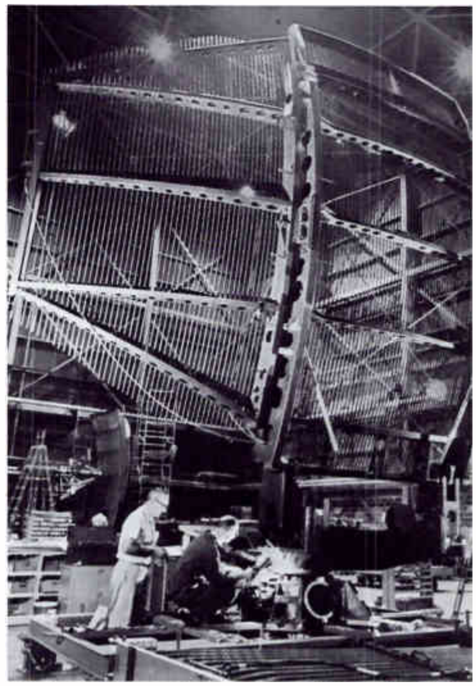

Shown in an advanced manufacturing stage is an antenna-microwave assembly of the new Air Force tactical ground-based radar system.

SF_6 Breaker Ratings Will Be Increased

Excellent installation, operation, and maintenance experience with the two-interrupter-module 362-kV and three-module 550-kV SF_6 circuit breakers has led to a development program aimed at producing a two-module 550-kV breaker by early 1970 and a three-module 765-kV breaker, both of simplified design, by late 1971. The breakers are products of the Westinghouse Power Circuit Breaker Division.

The higher-capacity interrupter mod-

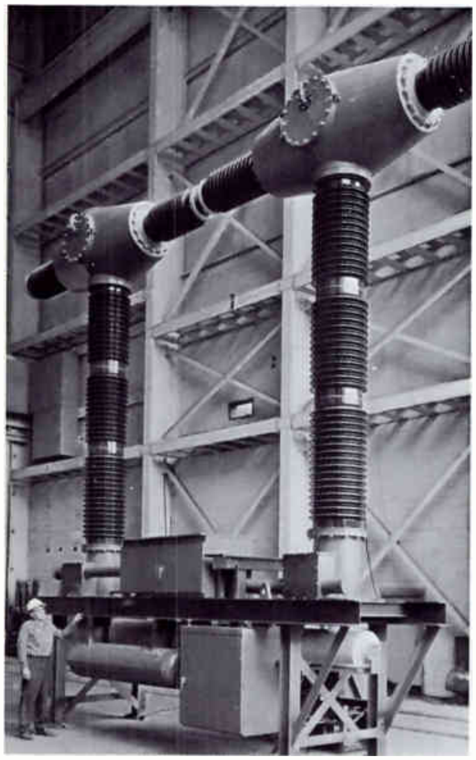

A 550-kV SF_6 circuit breaker with two interrupter modules being prepared for testing in the Westinghouse High Power Laboratory.

ule required will be similar to that now used, but contact travel and interrupter tank size will be slightly larger to provide the required dielectric strength across the open contacts. Entrance bushings will be longer also to handle the higher voltage applied per break.

Construction is being simplified in the new designs by eliminating the insulating guy structures now used with each column to provide required rigidity against wind and earthquake disturbances; a larger base support area and increased tension on the tie rods within the column will assure sufficient cantilever strength. Minor changes in the shock absorber and contact velocity control device, column tie and operating rod material, capacitor units, column base, and filter arrangements will further simplify installation and maintenance and increase reliability.

The excellent interrupting characteristics of SF_6 gas eliminate the need for shunting resistors on opening. A metallic resistor of revised design will be inserted in the circuit on breaker closing to control switching surges. Either a single-step or two-step resistor insertion sequence is available. A single step, as on the present breaker, probably will be used at 500 kV to control surges to a 2.0 p.u. level. At 765 kV, where control of surges to a maximum of 1.7 to 1.8 p.u. may be desired, a two-step resistor assembly can be provided. Computer studies show that this design is feasible, and that even lower maximum voltages of 1.5 p.u. can be obtained with two-step switching by selecting the instant on the voltage wave when the breaker's main contacts make.

Products for Industry

Submersible vacuum circuit breaker is a three-phase device consisting of a single stainless-steel housing and three mechanically ganged vacuum interrupters, each rated 600 amperes continuous. The interrupters are opened by a stored-energy mechanism that is spring operated and released by a shunt trip coil. The breaker is designed for operation at 15 kV maximum, 60 Hz, and it has a symmetrical interrupting capacity of 12,000 amperes and a basic insulation level of 95 kV. Weight is approximately 650 pounds. Sensing is accomplished by three current transformers. The reclosing switch is manually closed by either a handle or a rope-operated wheel. Manual tripping is provided by an overtoggle mechanism that is electrically and mechanically trip free. *Westinghouse Distribution Apparatus Division, P.O. Box 341, Bloomington, Indiana 47402.*

Solid-state frequency converter operates at optimum frequency for a given application, has efficiency of 90 to 95 percent, and has the inherent maintenance advantages of solid-state equipment. Model LF-250A 225-kW unit is continuously adjustable over entire 180- to 1000-Hz output frequency range and delivers full output power at any frequency within that range. Applications include induction heating for annealing, heat treating, hardening, melting, and mass heating. Load voltage is continuously adjustable from 20 to 100 percent. Input is three phase, 60 Hz, 460 volts, and output is single phase, 800 volts maximum. Units can be paralleled for increased power. *Westinghouse Industrial Equipment Division, P.O. Box 300, Sykesville, Maryland 21784.*

Air flow relay is a simple low-cost device for detecting air flow in equipment that depends on forced air for proper ventilation and cooling. A vane operates a relay when air movement ceases or drops below a preset level. Ratings are 15 amperes, 125 to 480 volts ac; ½ ampere, 125 volts dc; or ¼ ampere, 250 volts dc. Dimensions are 6⅞6 inches high by 3 inches wide by 2 inches deep, including the vane. The relay is available with normally open or normally closed contacts. *Westinghouse General Control Division, 4454 Genesee Street, P.O. Box 225, Buffalo, New York 14240.*

Gold-Line rectifier assemblies have guaranteed current rating, compact design, and wide range of standard current and voltage ratings. Applications include battery chargers, welders, power supplies, and communications equipment. The assemblies are available in nine frame sizes rated from 25 to 840 amperes, with various diode ratings and circuit configurations. Frames are for floor or wall mounting. *Westinghouse Semiconductor Division, Youngwood, Pennsylvania 15697.*

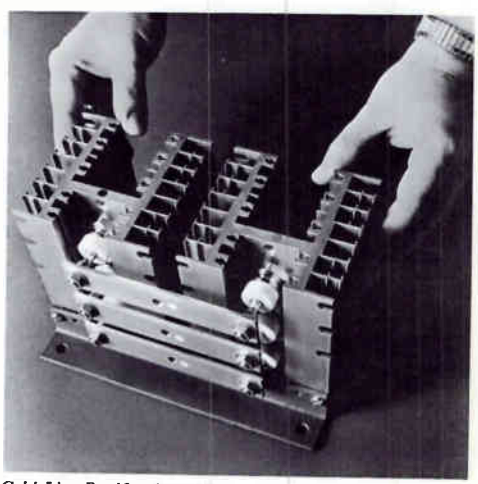

Gold-Line Rectifier Assembly

About the Authors

Calvin W. Eggers graduated from Valparaiso University in 1957 with a BSEE degree, and he received his MSEE degree from the University of Pittsburgh in 1960. He served as an instructor at Pitt and then joined Westinghouse in 1962 in the former Power Control Division, now a part of Hagan/Computer Systems Division. There he worked first in design and programming of computer systems for process-control and steel applications.

Eggers was project director for several power system automatic dispatching computers and then project director for the first digital automatic gauge control before going into engineering supervision. As Manager, General System Engineering, he is now responsible for a group concerned with application of power system computers and another group that applies Hagan analog control for steel and marine uses.

G. D. Rockefeller graduated from Lehigh University in 1948 with a BS in electrical engineering and went to work for Metropolitan Edison Company. He joined the Westinghouse Relay-Instrument Division in 1951, where his main responsibility has been the application and system design of protective relaying. Last year he received his MS degree from Newark College of Engineering.

Rockefeller has seven patents to his credit, and he has written texts on protective relaying and symmetrical components for International Correspondence Schools. He is a member of the Power System Relaying Committee of the IEEE Power Group.

Leo Husak was born in the Ukraine and came to the United States in 1951. He received his BSEE and MSEE degrees from Newark College of Engineering in 1957 and 1960, respectively.

Husak joined the Westinghouse Relay-Instrument Division in 1952. He worked first in application and then in the design section, where he has been concerned mainly with the design of high-speed distance relays.

Uno M. Elder earned his BSEE degree at the University of Colorado and has since taken graduate work at the University of Pittsburgh. He joined Westinghouse in 1940 in the former Motor Division at East Pittsburgh. Elder went into the Army in 1942 and spent the next three and a half years in a Signal Corps electronics training group, one of the liaison groups studying radar. He served as a radar officer, first attached to the Royal Air Force and then with the U.S. 313th Troop Carrier Group before and during the invasion of Europe.

Elder returned to Westinghouse, after the war, in the former DC Motor Engineering Department, where he had design responsibility at various times for the motors and generators in such specialty drives as those for elevators, machine tools, steel and paper mills, and mining equipment. He was made Supervisory Engineer in 1958, responsible for design and development of dc rotating equipment for special orders. Since 1962, he has been a Fellow Engineer with project engineer responsibilities. Projects he has directed include development of a dc motor with eight-to-one speed range for machine tools, a motor-generator set that successfully passed the U.S. Navy barge shock test on the first try, and the 800 MC motor line described in this issue.

Christie J. Photiadis graduated from the College of the City of New York in 1938 with a BS degree in chemistry. He then earned his MS in chemistry at the University of Minnesota and worked as a development chemist, first with Allied Chemical Corporation and then with Tidewater Oil Company. Photiadis joined Westinghouse in 1946 as a materials engineer in the Materials Engineering Department, working first on application of silicones to rotating equipment.

He moved to the Buffalo plant in 1948 to work on all phases of insulation development and application for motor and control apparatus. He is now a Senior Materials Engineer in the Large AC/DC Motor Division, working mainly in the application of plastics to motor insulation. He has contributed to development of Micarta tube winding techniques, high-temperature magnet coils, dielectric test methods, and the 800 MC and Life Line A and T motor lines.

C. J. Baldwin is Manager of Development, Advanced Systems Technology, Power Systems Planning Department. Besides being responsible for developing new digital computer applications for solving power systems problems, he manages Westinghouse consulting services for utility and industrial customers.

Baldwin joined Westinghouse in 1952 after earning his BSEE and MSEE degrees at the University of Texas. In 1956, he was awarded the Lamme Scholarship for a year of study at MIT; he graduated with a professional EE degree the following year.

Richard T. Byerly graduated from Texas A and M in 1948 with a BS in electrical engineering and then joined Westinghouse on the graduate student training program. He left the company to teach at the University of Pittsburgh, where he received his MS in electrical engineering in 1951. Byerly returned to Westinghouse in the Analytical Department in 1954. In 1957 he was named supervisor of a group applying digital computers to power systems analysis, and in 1963 he became an Advisory Engineer.

In his present post in Development, Advanced Systems Technology, Power Systems Planning, Byerly is responsible for automatic-control and power-systems analysis. He has contributed to the development of the analog economic dispatch computer, various major computer programs for the electric utility industry, and many special analytical studies such as calculation of the synchronous starting performance of the Seneca pumped-storage power generating plant.

Strips of "side-look radar" imagery are studied on a light table aboard a Westinghouse earth resources airplane. The two images were made by a radar system in the aircraft; they are different views of the same section of ground made from differently polarized return signals. The images reveal many terrain features, some of them clues to mineral presence, that cannot be found optically. For more information, see page 125.